AD NUMBER

AD019298

LIMITATION CHANGES

TO:

Approved for public release; distribution is unlimited.

FROM:

**Distribution authorized to U.S. Gov't. agencies and their contractors;
Administrative/Operational Use; 27 MAY 1953.
Other requests shall be referred to Naval Ordnance Test Station, Ballistics Division, Aerodynamics Branch, China Lake, CA.**

AUTHORITY

USNWC ltr dtd 23 Nov 1971

AD 19290

BLANK PAGES
IN THIS
DOCUMENT
WERE NOT
FILMED

TECHNICAL MEMORANDUM

NAVAL ORDNANCE TEST STATION

TM-998

THE ESTIMATION OF NORMAL FORCE AND PITCHING MOMENT COEFFICIENTS FOR BLUNT-BASED BODIES OF REVOLUTION AT LARGE ANGLES OF ATTACK.

by
HOWARD R. KELLY

RESEARCH DEPARTMENT

BALLISTICS DIVISION
AERODYNAMICS BRANCH

U. S. Naval Ordnance Test Station, Inyokern
China Lake, California

Local Project 701

27 May 1953

Prepared by:

Howard R. Kelly

HOWARD R. KELLY

FOREWORD

A systematic study of spin-stabilized rockets at the U. S. Naval Ordnance Test Station has provided, among other things, pitching moment and normal force coefficient data on short bodies of revolution. These data were for 5 , 7-, and 9-caliber body lengths at a Mach number of 0.26, and included runs with and without spin. An attempt to explain the nonlinear coefficients for angles of attack up to 30 degrees and with zero spin has resulted in the method presented here. The success of this theory at low speed prompted its extension to high speed flow. This study has been supported by NOTS Local Project LP 701.

This report has been reviewed for technical adequacy by Dr. Henry T. Nagamatsu, personal services contractor to NOTS, of the California Institute of Technology, Pasadena.

B. F. JAEGER
Head, Aerodynamics Branch

This memorandum is transmitted for information purposes only. It does not represent the official views or final judgment of the Naval Ordnance Test Station, and the Station assumes no responsibility for action taken on the basis of its contents.

CONTENTS

ABSTRACT

A method is developed which accurately predicts for blunt-based bodies of revolution the normal force coefficient and the pitching moment coefficient for angles of attack far beyond the range of potential theory. This method is based on the principle of superposition of the results of potential theory and the viscous force on a cylindrical body due to the transverse component of flow. In contrast to previously used methods, the viscous cross force is assumed not to be in a steady state, but in a transient development along the body.

This method is compared with experimental data for both subsonic and supersonic flows and with both laminar and turbulent axial boundary layer. The deviations between theory and experiment are in most cases an order of magnitude smaller than for a previous method due to Allen and Perkins.

INTRODUCTION

The aerodynamic design of aircraft rockets is somewhat unique in that the most practical body shape from other design considerations usually is a cylindrical shape with a blunt base and a moderately blunt nose. Very little good theoretical information is available on the lift and pitching moment for bodies of this type, except at very small pitching angles. For this reason, a considerable number of wind-tunnel tests have been made by the Naval Ordnance Test Station to build up a fund of information for design purposes.

While examining some of these data for the purpose of correlation between tests and with available theory, it was found that certain subsonic test data on short bodies at large angles of attack differed widely from any theoretical predictions available. The theory of Max Munk (Ref. 1) was found to give good results at small angles; this is satisfactory, since his is a linearized potential theory, and is not expected to be valid for large angles. A theory proposed by H. Julian Allen (Ref. 2), which has enjoyed a measure of success for supersonic flow data, grossly overestimates the effects of viscous crossflow at low subsonic speeds,

where it would at first be expected to be at its best.

The theory of Allen has been carefully examined, and a completely new version of his method is presented here. The problem of viscous crossflow has been reformulated with results quite different from his. His universal use of Munk's results for the linear potential theory contribution is questioned, and a revision of this policy is recommended. The results of a number of wind-tunnel tests by NOTS are presented in support of this new theory, showing excellent correlation. The predictions of Allen's theory are included for comparison, and the results of Munk's linear theory included as a sort of reference line, without intending a comparison.

This method is found to give formulas for certain cases that would appear to make it more difficult to use for engineering design purposes than Allen's method. It is shown, however, that considerable simplification can often be effected for this type of application, without seriously impairing the accuracy. An important result of this method is that it provides a means of extrapolating the results of tests at low Reynolds numbers, with

completely laminar boundary layer, to high Reynolds numbers, with fully developed turbulent boundary layers. This is a valuable asset for design work when test facilities are limited.

THEORY

Historical Development

The classical work of Munk (Ref. 1) is now so well known that the results of his theory may be quoted without detailed explanation. He found that the lift force distribution along the body of an airship is given by

$$dF = \frac{\rho U^2}{2}(k_2 - k_1)\frac{dS}{dx}\sin 2\alpha\, dx \qquad (1)$$

which integrates to zero along the body of the airship, but for a body of revolution with a flat base of area S_B, gives

$$L = \int dF = \frac{\rho U^2}{2}(k_2 - k_1)S_B \sin 2\alpha \qquad (2)$$

For a long slender body, $k_2 - k_1$ is almost unity, and if there is no boattail--so that the base area S_B is the reference area for defining lift coefficient--this coefficient is usually approximated as

$$C_L = 2\alpha \tag{3}$$

Munk realized that his linearized potential theory would apply only at small angles of attack, and that it would fail at large angles, chiefly due to viscous effects. There was apparently little interest at that time in developing a theory for large angles. Recently Allen (Ref. 2, 3, 4) has developed a method for predicting lift, pitching-moment, and the drag increment due to yaw, that has enjoyed considerable success with slender bodies of revolution at supersonic speeds.

Allen has assumed that the viscous contribution to lift is independent of the contribution of the potential flow, and writes the lift coefficient and pitching moment coefficient as the sum of two terms:

$$C_L = (k_2 - k_1)\frac{S_B}{A}\sin 2\alpha \cos\frac{\alpha}{2} + \eta C_{D_c}\frac{A_p}{A}\sin^2\alpha\cos\alpha \tag{4a}$$

$$C_M = \left[\frac{V - S_B(\ell - x_m)}{A}\right](k_2 - k_1)\sin 2\alpha\cos\frac{\alpha}{2}$$

$$+ \eta C_{D_c}\frac{A_p}{A}(x_m - x_c)\sin^2\alpha \tag{4b}$$

where the first term is always the result of Munk's theory, modified by the results of Ward (Ref. 5), who showed that the potential cross force is directed midway between the normal to the axis of revolution and the normal to the wind direction. Drag coefficient increments are not being treated in this report, so Allen's drag formula is omitted. The quantity C_{D_c} as used by Allen refers to the steady-state drag coefficient of an infinite cylinder in a flow normal to its axis. This was found by Allen to be $C_{D_c} = 1.2$ for a wide range of Reynolds numbers corresponding to the usual range of crossflow Reynolds numbers being considered. The factor η corrects this cylinder crossflow drag for the finite fineness ratio. Values of η have been tabulated by Goldstein (Ref. 6). The x_m is the (arbitrary) point about which pitching moments are measured; x_c is the axial position of the centroid of the planform area A_p, and the factor $\sin^2\alpha$ arises from the transformation of dynamic pressures from the cross velocity $V \sin\alpha$ to the free stream velocity V.

Since his theory is only approximate, Allen simplified his formulas by making the approximations $\sin\alpha = \alpha$, $k_2 - k_1 = 1$, $\cos\alpha = 1$. This results in

$$C_L = 2\left(\frac{S_B}{A}\right)\alpha + \eta C_{D_c}\left(\frac{A_p}{A}\right)\alpha^2 \qquad (5a)$$

$$C_M = 2\left[\frac{V - S_B(\ell - x_m)}{A}\right]\alpha + \eta C_{D_c}\left(\frac{A_p}{A}\right)(x_m - x_c)\alpha^2 \qquad (5b)$$

and his theory is used in essentially this form. J. A. F. Hill at the Naval Supersonic Laboratory, Massachusetts Institute of Technology, used Allen's results in 1950 (Ref. 7), but modified them to include boundary layer displacement thickness in the potential theory term, thus changing the effective values of both S_B and V. He also observed that Allen's assumed value of $C_{D_c} = 1.2$ is not appropriate if the axial boundary layer is turbulent, even though the crossflow Reynolds number corresponds to a laminar boundary layer.

The Viscous Cross Flow

In the theory presented in this paper we shall replace the use of the lift coefficient C_L by the normal force coefficient C_N. This will not change the first (potential theory) term of equation 4a, and will eliminate the factor of cos α in the second (viscous) term of this equation. It also eliminates the necessity of Allen's assumption that the component of axial drag involved in the lift force may be neglected. This assumption would be invalid for the angular range of interest here. As Hill has pointed out in Ref. 7, Allen's equation (5a) would be more appropriate for the normal force coefficient C_N for comparison purposes here.

Allen's fundamental equation for the viscous cross flow is apparently quite correct if properly interpreted. He writes the viscous contribution to the cross force from a cylindrical element of length dx as

$$dF = 2rC_{D_c} \frac{\rho V_c^2}{2} dx \qquad (6)$$

where r is the body radius at the point x, and V_c is the cross velocity, as shown in Fig. 1. The quantity ρ is the usual mass density, and C_{D_c} is the drag coefficient of a circular cylinder at the Reynolds number

$$Re_c = \frac{2rV_c}{\nu} \tag{7a}$$

and the Mach number

$$M_c = \frac{V_c}{a} \tag{7b}$$

with the kinematic viscosity ν and speed of sound a evaluated in the undisturbed flow. Then, since

$$V_c = U \sin\alpha \tag{7c}$$

it follows that

$$dF = 2rC_{D_c} q \sin^2\alpha \, dx \tag{8}$$

in terms of the dynamic pressure $q = \frac{\rho U^2}{2}$ of the free stream.

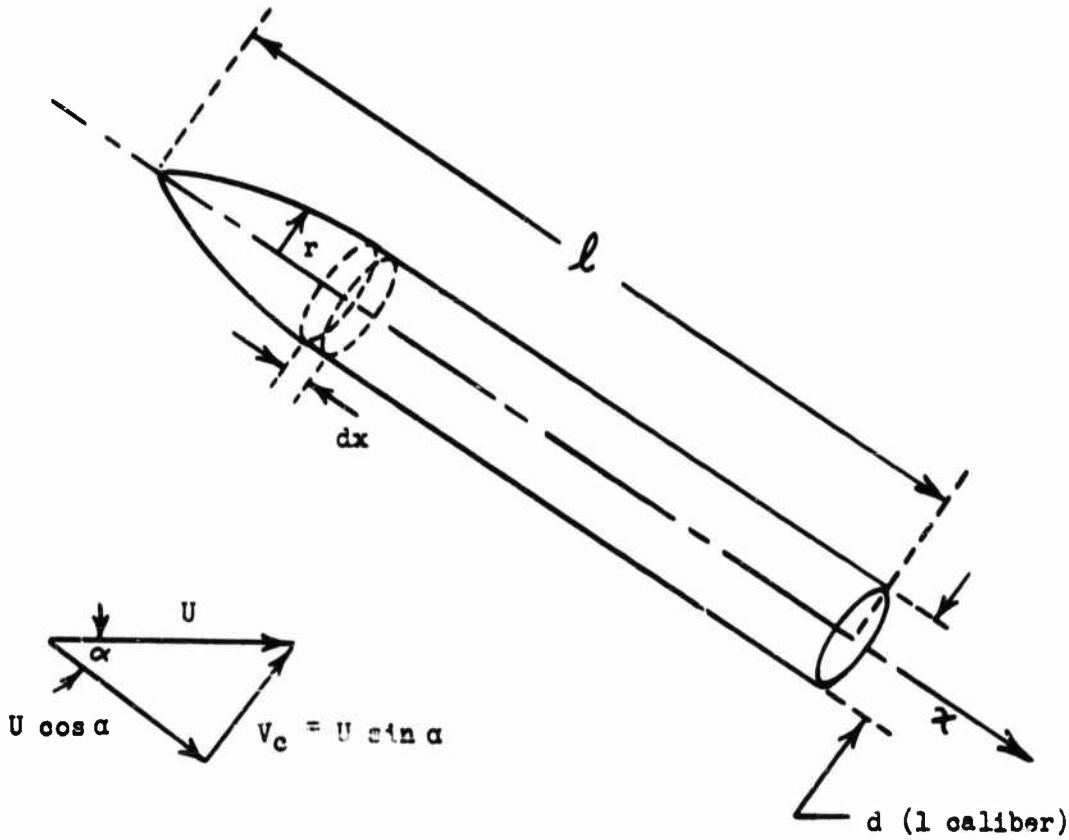

FIG. 1. GEOMETRY FOR BODY OF REVOLUTION
WITH ANGLE OF ATTACK α .

Since the drag coefficient of a circular cylinder in a cross flow is usually given for the two-dimensional case of an infinite cylinder, Allen adds a parameter η, which represents the reduction in drag coefficient of a cylinder due to its finite length. Then if the moment coefficient for a body of diameter d, referred to a point x_m,

$$C_M = \frac{M_p}{qAd} \tag{9a}$$

and the normal force coefficient

$$C_N = \frac{N}{qA} \tag{9b}$$

we find the increments in these coefficients, due to viscosity, to be

$$\Delta C_N = \frac{2\,\eta \sin^2 \alpha}{A} \int_0^{\ell} r C_{D_c} dx \tag{10a}$$

and

$$\Delta C_M = \frac{2\,\eta \sin^2 \alpha}{Ad} \int_0^{\ell} r C_{D_c} (x_m - x) dx \tag{10b}$$

which lead to the final terms of equations (4a) and (4b). These terms are entirely due to viscous effects, since C_{D_c} always vanishes for a true potential flow.

Evaluation of Parameters

The departure of the theory of this report from that of Allen lies principally in the evaluation of the parameters of equations (10) and of the potential theory. It was well known to both Allen and Hill that the coefficient C_{D_c} should not be the steady state drag coefficient, as used by them, but should be related to the transient effect found by Schwabe (Ref. 8). The results of Schwabe's experiments are reproduced here as Fig. 2. This curve represents the drag coefficient for a circular cylinder moving crosswise in a fluid when started impulsively from rest, as computed from the observed flows. For a cylinder of radius r_1, it is found that the drag coefficient rises rapidly from zero until the parameter $\frac{V_c t}{r_1}$ is about 4. A very slow increase continues until, when this parameter reaches a value of 9, the drag coefficient is 2.07, or twice the steady-state value of about 1.0 for the Reynolds number of the experiment.

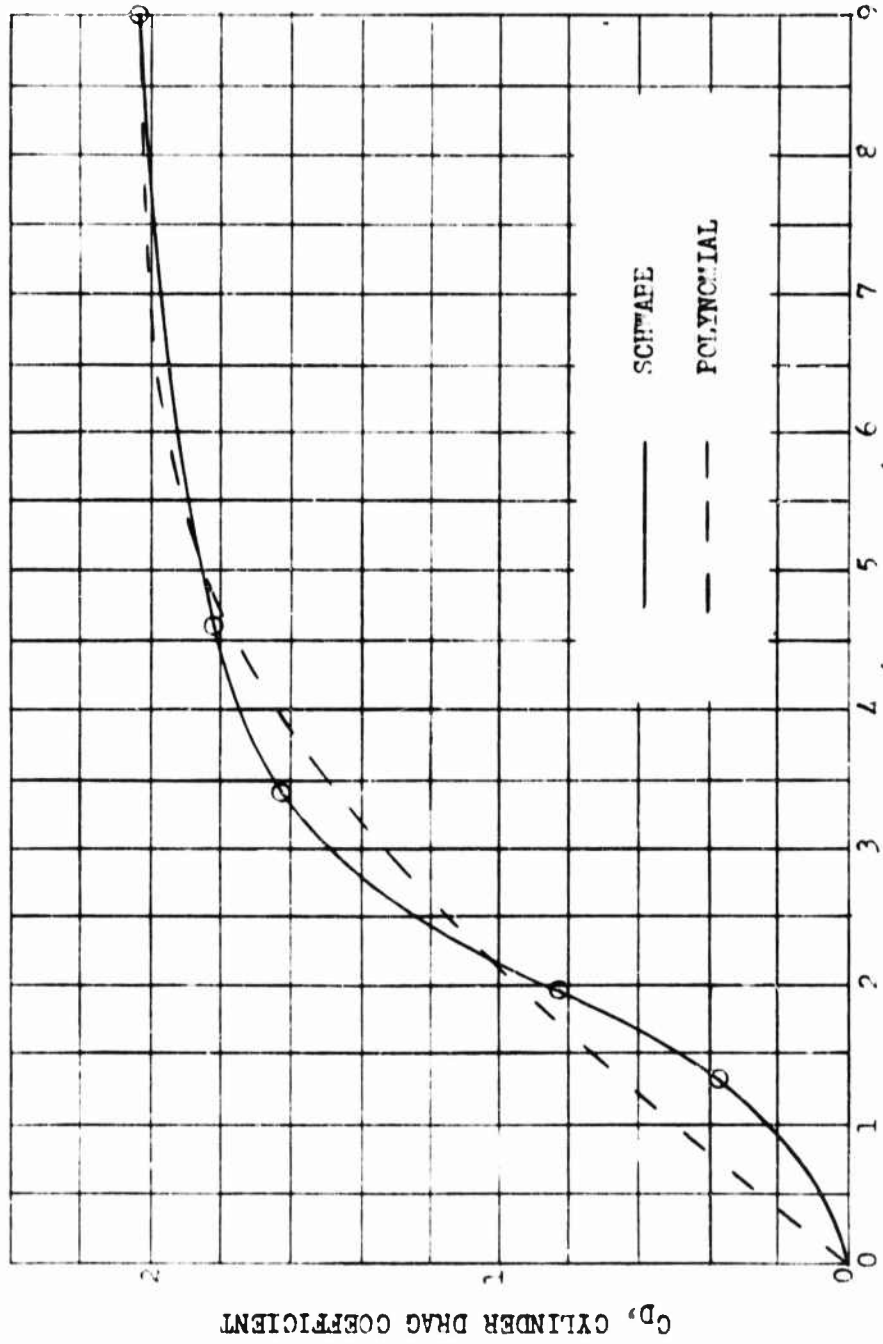

FIG. 2. APPROXIMATION OF SCHWABE'S RESULTS BY A FIFTH DEGREE POLYNOMIAL.

Referring to Fig. 1, we may consider a plane lamina of air of thickness dx moving along the body axis with speed U cos α and across the body with speed U sin α. At the nose of the body, this lamina suddenly begins to flow about a circular cylinder of variable radius r. A potential cross flow will exist at the nose, with a gradual development of viscous cross flow along the body. Schwabe's parameter becomes

$$\frac{V_c}{r} t = \frac{U \sin \alpha}{r} \frac{x}{U \cos \alpha} = \frac{x}{r} \tan \alpha \qquad (11)$$

In order that equations (10) may be integrated readily, it is advisable to approximate Schwabe's results by a simple function. This function was first chosen to be a linear increase of drag coefficient from 0 at $\frac{V_c t}{r} = 0$ to 2.0 at $\frac{V_c t}{r} = 4$, and to remain constant at 2.0 until $\frac{V_c t}{r} = 9$. No information is given by Schwabe of the transition back to the steady state for larger values of his parameter. It may be seen from Fig. 3, however, that this parameter range covers most body lengths and angles of attack of practical interest.

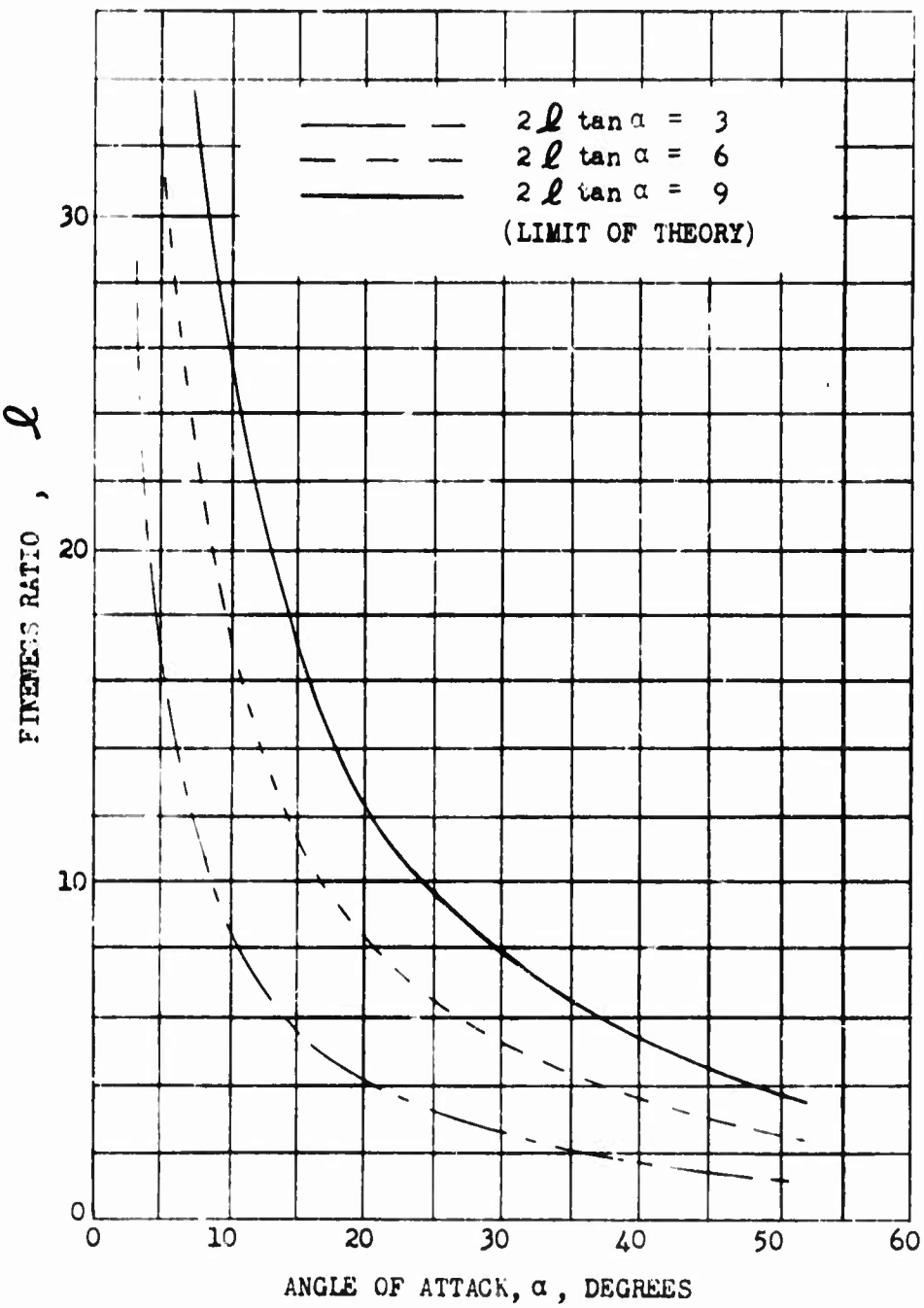

FIG. 3. RANGE OF APPLICATION OF PRESENT THEORY.

The linear approximation works quite well, but yields unwieldy expressions for angles greater than that for which $\ell \tan \alpha = 2$, since the factor $\tan \alpha$ appears as a limit of integration. The experimental curve by Schwabe resembles a portion of an arc tangent curve, which suggests the use of such a function. The evaluation of the integrals obtained appears to yield more complicated formulas than the present problem deserves. The Taylor expansion of an arc tangent function

$$y = \tan^{-1} x = x \quad \frac{x^3}{3} + \frac{x^5}{5} + \quad - - \qquad (12)$$

suggests that the same result may be obtained by integrating term by term, except that the factors containing $\tan \alpha$ separate out immediately this way. The limits of applicability of this theory, due to a change in flow conditions at large angles, renders the use of terms beyond the fifth power questionable, so that a truncated arc tangent of the form

$$C_{D_c} = A' \frac{x}{r} \tan \alpha + B' \frac{x^3}{r^3} \tan^3 \alpha + C' \frac{x^5}{r^5} \tan^5 \alpha + \quad - - - \qquad (13)$$

will be sufficient for practical purposes.

The cylinder cross flow drag function may be integrated for specific body shapes. Since the integral is multiplied by $\sin^2\alpha$, we may simplify the results by using

$$\sin^2\alpha \tan\alpha = \alpha^3 + \frac{\alpha^7}{15} + - - - \tag{14a}$$

$$\sin^2\alpha \tan^3\alpha = \alpha^5 + \frac{2\alpha^7}{3} + - - - \tag{14b}$$

$$\sin^2\alpha \tan^5\alpha = \alpha^7 + - - - \tag{14c}$$

so that, to terms in α^7, the normal force and moment coefficient increments will be of the form

$$\Delta C_N = \frac{2C_{D_c}}{A}[D_N\alpha^3 + E_N\alpha^5 + F_N\alpha^7] \tag{15a}$$

$$\Delta C_M = \frac{2C_{D_c}}{A}[D_M\alpha^3 + E_M\alpha^5 + F_M\alpha^7] \tag{15b}$$

where C_{D_c} is the steady-state value of the cylinder cross flow drag coefficient. The particular functions obtained for some typical body shapes will be derived in Appendix A. It has been

found that the linear term in Eq. 13, leading to a cubic in normal force coefficient and moment coefficient, is sufficiently accurate for much of the data in this report.

It is also necessary to choose an appropriate value of the parameter η for the transient phenomenon being considered. The fact that η is different from unity for the steady state is principally due to the distortion of flow near the ends of a cylindrical body. A lamina of fluid will not remain in a plane, but will flow in such a way that the total flow will meet less resistance. In the case of the transient development being considered for a blunt-based body of revolution, this effect will not have time to develop at the base before the flow leaves the body. A distortion may develop at the nose, but the viscous force contribution at the nose is very small, and the effect may usually be neglected. For these reasons, the factor η will be replaced by unity.

If a body does not have a blunt base, that is has boattail, the above argument will fail, since considerable distortion of the cross flow planes will occur in a region where the viscous effects

are greatest. For this case, the value of η may differ significantly from unity, which is one reason the present report is restricted to blunt-based bodies.

An interesting feature of the results in Eq. 15 is that the expressions for the coefficients become odd functions, so apply directly to both positive and negative angles. Allen's quadratic formulas can only apply to negative angles of attack if they are considered to represent absolute values of the coefficients.

There remains the problem of determining the appropriate value of $(k_2 - k_1)$, the factor in Munk's theory representing the difference in apparent mass for longitudinal and transverse motion of the body. Munk includes a table of values of $k_2 - k_1$, originally computed by Lamb (Ref. 9, p. 155). These values were computed for ellipsoids of revolution, but do not necessarily apply to cone-cylinder or ogive cylinder combinations of the same fineness ratio. Munk states that the values may be used for airship design if the ellipsoid has the same length and volume, or if Volume/ℓ^3 has the same value. This will not be as good an approximation for a cone-cylinder, but in the absence of better methods will serve as a method for correcting what is

already a correction factor. As an example of the difference this correction makes for short bodies, a cone-cylinder of 5 caliber total length and 2 caliber head length is found to be equivalent to an ellipsoid of 11 calibers total length. The value of $k_2 - k_1$ for 5 calibers is 0.836, while for 11 calibers it is 0.95. Experimental evidence favors the latter value.

Boundary Layer Corrections

Hill has pointed out in Ref. 7 that the boundary layer may necessitate two corrections to the theory of Allen, one in the viscous flow term, and one in the potential term. His modified form of Allen's theory does not eliminate the fundamental difficulty and principal source of error, but this type of correction may not in general be neglected in a precise theory.

Allen's viscous cross flow term assumes that the cross flow is completely independent of the axial flow, and will therefore depend only on the cross flow Reynolds number (Eq. 7a) and Mach Number (Eq. 7b). There is good experimental evidence, however (Ref. 6, p. 431), that the critical Reynolds number for the decrease of the drag coefficient of a cylinder from the laminar

flow value to the turbulent flow value changes rapidly with the turbulence level present in the stream. It seems logical that if a cross flow in this range of Reynolds numbers encounters a turbulent axial boundary layer, that the proper drag coefficient C_{D_c} to use will be that for a turbulent cross flow. The coefficient appears to change by a factor of about 3, and the steady state values of C_{D_c} that will be used here will be 1.2 for the case of completely laminar boundary layer, and 0.35 for (almost) completely turbulent boundary layer.

The effect of boundary layer on the potential theory term arises from the fact that the flow is displaced as though the body shape were changed. In particular, the effective base area S_B and volume V will be greater. The important boundary layer parameter will be the displacement thickness

$$\delta^* = \int_0^{\delta} (1 - \frac{u}{U})dy \qquad (16)$$

For laminar boundary layer this thickness may be found approximately from

$$\frac{\delta^*}{x} = \frac{\Delta}{\sqrt{Re}} \tag{17}$$

where

$$\Delta = 1.73 + 0.48M^2 \tag{18}$$

The turbulent boundary layer displacement thickness, as shown by Prandtl from the seventh power law

$$\frac{u}{U} = \left(\frac{y}{\delta}\right)^{\frac{1}{7}} \tag{19}$$

is given by

$$\frac{\delta^*}{x} = \frac{K}{(Re)^{0.2}} \tag{20}$$

where K = 0.046 for incompressible flow on a flat plate. Flat plate data from the Daingerfield supersonic wind tunnel indicate an approximate value of K = 0.08 for a Mach number of 1.56, which is of interest in this report. Hill has computed the

fractional increase in base area from S_B to S_B' and approximate formulas for the fractional increase in volume from V to V', based on the assumption of constant diameter and fully turbulent boundary layer. These are, for the laminar case

$$\frac{S_B'}{S_B} - 1 = 4\frac{\Delta}{\sqrt{Re_d}}\sqrt{\frac{\ell}{d}}\left[1 + \frac{\delta}{\sqrt{Re_d}}\sqrt{\frac{\ell}{d}}\right] \qquad (21)$$

$$\frac{V'}{V} - 1 = \frac{2}{3}\frac{\pi d^3}{V}\frac{\Delta}{\sqrt{Re_d}}\left(\frac{\ell}{d}\right)^{\frac{3}{2}}\left[1 + \frac{3}{4}\frac{\Delta}{\sqrt{Re_d}}\sqrt{\frac{\ell}{d}}\right] \qquad (22)$$

and for the turbulent case

$$\frac{S_B'}{S_B} - 1 = 4\frac{K}{(Re_d)^{0.2}}\left(\frac{\ell}{d}\right)^{0.8}\left[1 + \frac{K}{(Re_d)^{0.2}}\left(\frac{\ell}{d}\right)^{0.8}\right] \qquad (23)$$

$$\frac{V'}{V} - 1 = \frac{5}{9}\frac{K}{(Re_d)^{0.2}}\left(\frac{\ell}{d}\right)^{1.8}\left[1 + \frac{9}{13}\frac{K}{(Re_d)^{0.2}}\left(\frac{\ell}{d}\right)^{0.8}\right] \qquad (24)$$

Supersonic Potential Flow

Allen has assumed that the normal force and pitching moment may be found by the simple addition of the potential flow solution and the viscous cross flow solution. The logical application of this principle will use the best available potential flow solution. For subsonic flow, the theory of Munk, corrected for boundary layer, gives excellent results. For supersonic flow, however, Munk's theory does not apply, except possibly in the limiting case of bodies with extremely long, slender noses.

A much better approximation to the potential flow solution for supersonic flows is obtained by the second-order theory of Van Dyke (Ref. 10). This theory has been applied recently to the calculation of pressure distributions, normal force coefficients, and pitching moment coefficients for a series of tangent-ogive-cylinder combinations (Ref. 11). These must necessarily be computed for a finite number of discrete supersonic Mach numbers, so a method of interpolation is desirable In Fig. 4 and 5, the values of $dC_N/d\alpha$ and $dC_M/d\alpha$ for $\alpha = 0$ degrees as computed in Ref. 11 are plotted as a function of $\beta = \sqrt{M^2 - 1}$

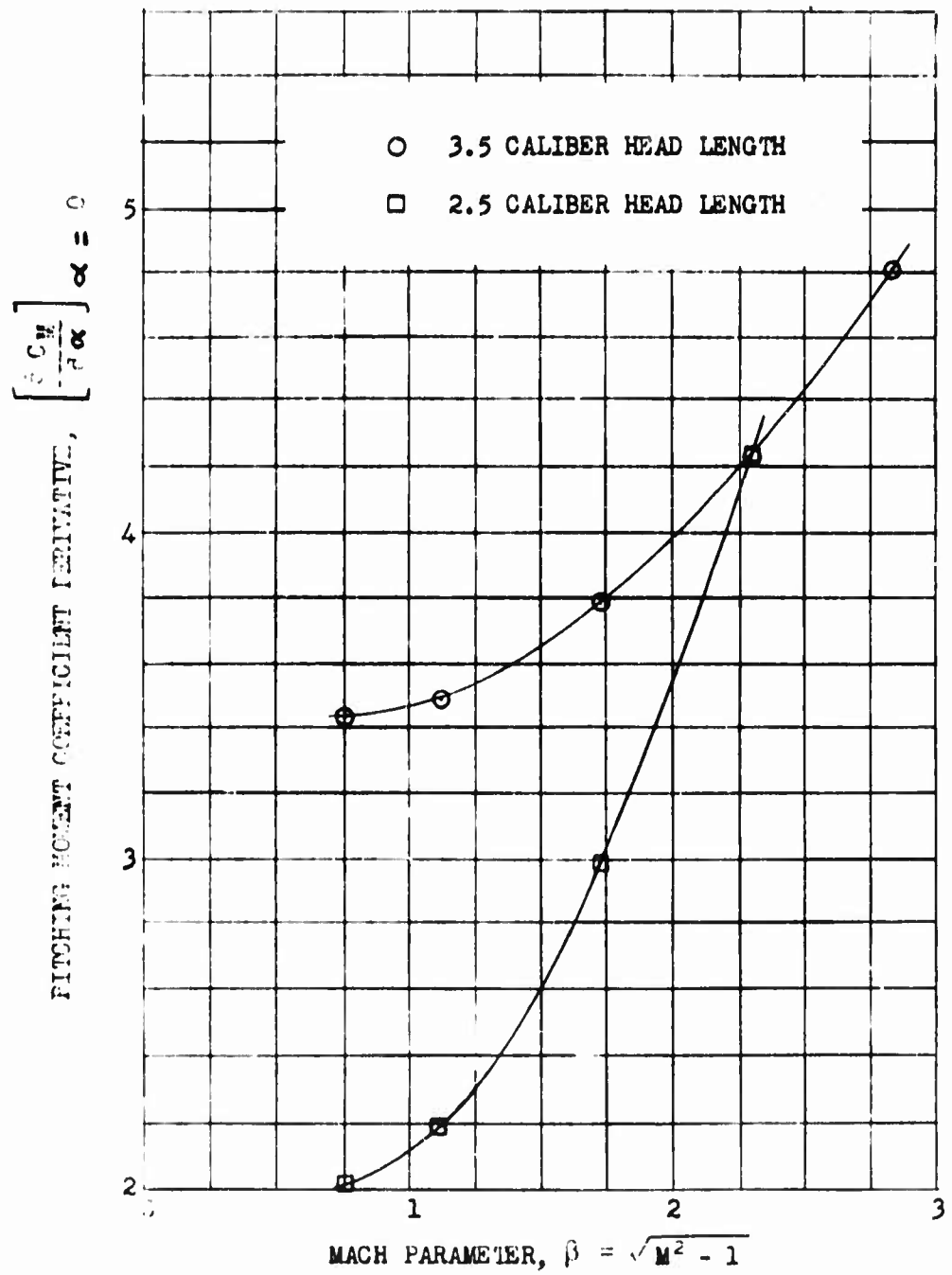

FIG. 4. INITIAL SLOPE OF COEFFICIENT OF PITCHING MOMENT (ABOUT NOSE) FROM VAN DYKE THEORY, $\ell = 14$.

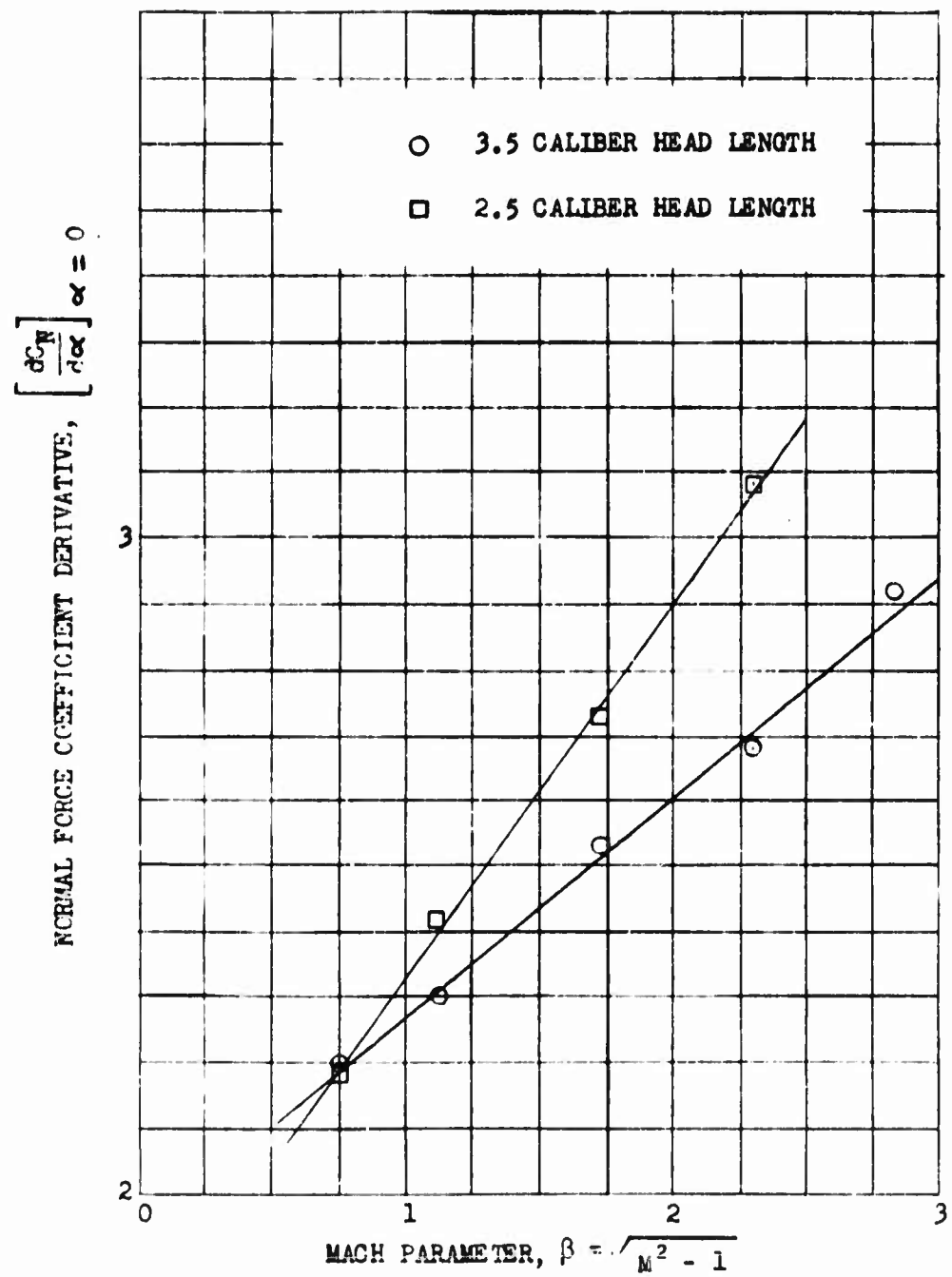

FIG. 5. INITIAL SLOPE OF COEFFICIENT OF NORMAL FORCE FROM VAN DYKE THEORY, $\ell = 14$.

with ogival head length as a parameter. These values were computed for a total body length of 14 calibers, and do not change appreciably with increase in body length beyond 9 calibers. It may be seen that interpolation may be made along smooth curves for the moment coefficient slope, while the interpolation is linear for the normal force coefficient slope. No particular significance has been attached to this linear relation, except for a convenient method of interpolation.

EXPERIMENTAL VERIFICATION

The theory described above is compared with Allen's method and with experimental data in Appendix B, Fig. 6-19. The extrapolation of Munk's linear potential theory in the form $C_N = 2\alpha$ and $C_{M_B} = \frac{2V}{A}\alpha$ is included as a reference line for demonstration of nonlinearity. The exact body shape was not used in computing theoretical results. For the tangent ogives, the circular arc was approximated by a parabolic arc, as explained in Appendix A. The secant ogives for the short bodies were approximated by cones. The contribution to the viscous cross force from the head is so small that the error involved in these approximations is negligible.

Short Bodies in Subsonic Flow, With Turbulent Boundary Layer

The moment coefficient for the 5 caliber body (Fig. 6) shows very little nonlinearity up to 20 degrees, but in the range from 20 to 30 degrees a slight curvature is shown. The agreement with experimental data is everywhere excellent. Allen's method grossly overestimates the nonlinear effects. The normal force coefficient (Fig. 7) shows a similar agreement between the present theory and experiment, with overestimation by Allen's method. No definite conclusions may be drawn from the center of pressure, except that both nonlinear theories predict the rearward shift with large angles of attack.

The moment coefficient (Fig. 8) and the normal force coefficient (Fig. 9) for the 7 caliber body again show an excellent agreement between the present theory and experiment, Allen's method again being high. The center of pressure shows a larger rearward shift with angle, with slightly better agreement for the present theory than for Allen's method.

The correlation of the present theory with experiment for the 9 caliber length is also remarkably good (Fig. 10, 11). The results for center of pressure are more distinct in this case.

Comparing the low-angle results here with those in Fig. 7 and Fig 9, it seems likely that the boundary layer corrections are inadequate. This deviation is not serious, however, considering the sensitivity of center of pressure to small errors in forces and moments.

It is noteworthy that Allen's method, based on subsonic theory and data, shows a greater deviation from experiment at these low speeds than for low supersonic speeds. It may be argued that it is not a fair comparison to correct for the apparent mass factor, boundary layer thickness, and for the fact that $\sin 2\alpha$ differs from 2α in presenting the results of the present theory, but not in Allen's formula. Such corrections in Allen's formula, however, would account for only a small part of the error shown, and the formula is used just as used for large angles by Allen and Perkins (Ref. 4).

Turbulent Boundary Layer at Supersonic Speed

Data are presented for three different bodies of revolution at a Mach number M = 1.56 in Fig. 12 17. The Reynolds numbers for these tests were such that the boundary layer was probably

turbulent for most of the body length, except for the 10 caliber model. Schlieren pictures have indicated a boundary layer transition about 5 calibers from the nose.

The agreement with experiment is better on the average for the present theory than for Allen's method. The apparent agreement between his method and the data is probably fortuitous, being the result of two or more errors tending to cancel. This is especially true for the longer bodies, where the initial slope for the experimental data is considerably greater than for Allen's theory, which has the same initial slope as the linear potential theory.

The agreement between the present theory and experiment is good for center of pressure, where deviations of the order of half a caliber may be within experimental error.

Laminar Boundary Layer at Supersonic Speed

One body shape has been selected for which the boundary layer probably remains laminar at the test Mach number of 2.87 and Reynolds number of 3.72 million. It was also chosen because Van Dyke's second order theory applies to it at this high Mach number. For this body, of length 14 calibers and head length

3.5 calibers, the corrections for displacement thickness of the laminar boundary layer are small compared to the turbulent thickness at Mach 1.56, but are included for completeness. The value $C_{D_c} = 1.2$ is used in contrast to $C_{D_c} = 0.35$ for all the previous curves.

The failure of Allen's formula is quite apparent in Fig. 18 and 19. For the true laminar case shown, his combination of subsonic potential theory and quadratic viscous term falls far short of the experimental data, even for angles up to 8 degrees. A comparison of Fig. 18 and 19 with Fig. 16 and 17 shows the striking difference in nonlinear effects between laminar and turbulent boundary layers.

PRACTICAL ENGINEERING APPLICATION

It has been shown that the present theory agrees well with experimental data over a wide range of Mach numbers, Reynolds numbers, and body shapes. For practical use, it is desirable to be able to simplify the equations whenever possible. The complete equations may be given as

$$C_N = \left(\frac{dC_N}{d\alpha}\right)_{\alpha = 0} \sin\alpha \cos\alpha \cos\frac{\alpha}{2} + \frac{2C_{D_c}}{A}[D_N\alpha^3 + E_N\alpha^5 + F_N\alpha^7] \quad (25a)$$

$$C_M = \left(\frac{dC_M}{d\alpha}\right)_{\alpha = 0} \sin\alpha \cos\alpha \cos\frac{\alpha}{2} + \frac{2C_{D_c}}{A}[D_M\alpha^3 + E_M\alpha^5 + F_M\alpha^7] \quad (25b)$$

The $\frac{dC_N}{d\alpha}$ and $\frac{dC_M}{d\alpha}$ are given by Munk's theory at subsonic speeds, after correcting for the apparent mass factor and the boundary layer thickness, and for supersonic speeds are found from Van Dyke's second order theory, with boundary layer corrections added. The D, E, F coefficients are computed as shown in Appendix A, and C_{D_c} is 1.2 or 0.35 as the axial boundary layer is laminar or turbulent, respectively.

Figure 20 shows a comparison of the normal force coefficient C_N, as computed by the complete equation with various approximations, for the 9 caliber length body at subsonic speeds. It is found that the combined corrections for boundary layer thickness and apparent mass factor may be omitted for this case with little loss in accuracy. These corrections tend to cancel, and are of the same order of magnitude for body lengths of 5 to 7 calibers.

For very short bodies the $(k_2 - k_1)$ factor will dominate and for very long bodies, with $k_2 - k_1 \cong 1$, the boundary layer correction will become important.

The use of $2 \sin\alpha \cos\alpha \cos\frac{\alpha}{2} \equiv \sin 2\alpha \cos\frac{\alpha}{2} \cong 2\alpha$ is shown to be valid up to 10 degrees, and has been used this way for all figures for which the angle of attack α was less than 8 degrees. Approximations obtained by dropping the seventh power term, or both fifth and seventh powers, show that the cubic equation is quite accurate for $2\ell \tan\alpha \leq 3$, the quintic equation holds to $2\ell \tan\alpha = 6$, and the seventh power is good to $2\ell \tan\alpha = 9$, the limit of application of this theory (see Fig. 3).

The case of turbulent axial boundary layer in supersonic flow is shown in Fig. 21. Normal force coefficients are plotted for a 14 caliber length body with 2.5 caliber nose length for the complete equation (but with $\sin 2\alpha = 2\alpha$) and with approximate formulas. The neglect of boundary layer thickness begins to be significant, if an accurate estimate of normal force is desired, but may be sufficiently good for rough estimation purposes. The curves are approximated very well by a cubic equation, in agreement with the criterion of the last paragraph. The errors due to boundary

layer thickness will increase with Mach number and body length, and the errors due to shortening the polynomial expression increase with body length, for a given angle of attack.

Comparisons are also made for the case of laminar boundary layer (Fig. 22) on a 14 caliber body. The results of shortening the polynomial are similar to those found in the last paragraph. For the laminar boundary layer, the effects of displacement thickness are small in comparison with similar effects of a turbulent boundary layer, and may usually be neglected.

It is found that for a special case of subsonic flow, with moderate length bodies and $\alpha \leq 10$ degrees, the formulas

$$C_N = 2\alpha + 0.49\frac{C_{D_c}\ell^2}{A}\alpha^3 \qquad (26a)$$

$$C_{M_B} = \frac{2V}{A}\alpha + 0.49\frac{C_{D_c}\ell^3}{3A}\alpha^3 \qquad (26b)$$

where $D_N = 0.49\frac{\ell^2}{2}$, $D_M = 0.49\frac{\ell^3}{6}$ have been substituted, give good approximations to the normal force and pitching moment coefficients. These formulas will not always be sufficient for large angles, very long bodies, for supersonic flows,

or for the case of very thick turbulent boundary layer, but the corrections for these cases are usually simple to apply. The value of C_{D_c} must be chosen as 1.2 or 0.35 as the axial boundary layer is laminar or turbulent, respectively.

In the case of supersonic flow, there are some body shapes and Mach numbers for which Van Dyke's theory does not apply. This theory is still useful if experimental data at small angles of attack are available. Slopes $\frac{dC_N}{d\alpha}$ and $\frac{dC_M}{d\alpha}$ at $\alpha = 0$ may be measured and used in Eq 25 in place of the slopes from Van Dyke's theory. This technique will be valuable in extrapolating wind tunnel data for small models to free-flight conditions with large models. Care should be taken to note the boundary layer conditions of the wind tunnel tests and free-flight applications.

CONCLUSION

A method has been developed for the estimation of normal force coefficients and pitching moment coefficients for blunt-based bodies of revolution at large yaws. The equations reduce to

$$C_N = 2\alpha + 0.49 \frac{C_{D_c} \ell^2}{A} \alpha^3$$

$$C_{M_B} = \frac{2V}{A}\alpha + 0.49 \frac{C_{D_c} \ell^2}{3A} \alpha^3$$

for subsonic speeds if $\alpha \leq 10$ degrees, $2\ell \tan\alpha \leq 3$, as long as the boundary layer thickness does not increase the base area appreciably. Van Dyke's theory should be used for the linear term in supersonic flow, and a higher order polynomial is needed if $2\ell \tan\alpha \geq 3$.

The method is also useful for extrapolation of small-yaw data to large yaws and to different Reynolds numbers. As far as is known, this is the first adequate theory that has been developed for this purpose.

The results presented here have only been applied in the Mach number range from M = 0 to M = 2.87 and for a limited range of Reynolds numbers. Further investigation will be made, especially in the high Mach number range. The results of a more complete investigation will be described in a later report.

Appendix A

CALCULATION OF NONLINEAR TERMS

The experimental measurement by Schwabe of the development of cross drag coefficient for a circular cylinder (Fig. 2) resembles an arc tangent function, except at small values of the argument, where contributions to normal force in the present theory will usually be quite small in comparison with the linear term. The arc tangent function may be integrated directly, but results in complicated formulas. A Taylor expansion of the arc tangent, which is an infinite series containing only odd powers, converges quite slowly. Such a series may be truncated, however, so that it represents the function over a limited range of the argument with the use of a few of the leading terms, if the coefficients of these terms are properly adjusted. The representation of Schwabe's data was chosen to be of the form

$$C_{D_c} = A' \frac{x}{r} \tan\alpha + B' \frac{x^3}{r^3} \tan^3\alpha + C' \frac{x^5}{r^5} \tan^5\alpha \qquad (1A)$$

By a least squares procedure, A', B', and C' were evaluated giving

$$C_{D_c} = 0.49\frac{x}{r}\tan\alpha - 0.0056\frac{x^3}{r^3}\tan^3\alpha + 0.00003\frac{x^5}{r^5}\tan^5\alpha \qquad (2A)$$

This function is compared with Schwabe's data in Fig 2.

For computation of viscous cross flow effects, one must evaluate the integrals in the expressions

$$\Delta C_N = \frac{2}{A}\sin^2\alpha\int_0^{\ell} r\, C_{D_c}\, dx \qquad (3A)$$

$$\Delta C_M = \frac{2}{A}\sin^2\alpha\int_0^{\ell} r\, C_{D_c}\,(x_m - x)dx \qquad (4A)$$

where C_{D_c} is given by (1A) multiplied by the steady-state value, since the steady state value in Schwabe's experiment was about unity. This procedure assumes that the shape of the curve found by Schwabe always applies, and only the absolute magnitudes change with Reynolds number. These integrations have been carried out for bodies with conical and parabolic ogival heads on

cylindrical bodies, where the body length is ℓ calibers and the head length is h calibers. The radius r for the generating curves of the heads are given by

$$r = \frac{x}{2h} \tag{5A}$$

calibers for the cone and

$$r = \frac{x}{h} - \frac{x^2}{2h^2} \tag{6A}$$

for the parabola. The parabola is a close approximation to a circular tangent ogive, and is much simpler to integrate than the exact function.

It is sufficient to perform the integrations for the case of a steady state C_{D_c} of unity, and apply a correction factor outside the integral. The integral for the normal force coefficient for a cone-cylinder is

$$\int_o^{\ell} r\, C_{D_c}\, dx = A' \frac{\ell^2}{2} \tan\alpha + B'[\ell^4 + h^4]\tan^3\alpha + 16C'[\frac{\ell^6}{6} + \frac{h^6}{3}]\tan^5\alpha \tag{7A}$$

and for a parabolic-ogive-cylinder

$$\int_0^{\ell} r\, C_{D_c}\, dx = A' \frac{\ell^2}{2} \tan \quad + B' [\ell^4 + \frac{3h^4}{4} + \log 2] \tan^3 \alpha$$

$$+ 16C' [\frac{\ell^6}{6} + \frac{h^4}{24}] \tan^5 \alpha \qquad (8A)$$

For the moment coefficients about a point x_m calibers from the nose of he body, the integral for the cone-cylinder is

$$\int_0^{\ell} r\, C_{D_c} (x_m - x) dx = A' [\frac{\ell^2 x_m}{2} - \frac{\ell^3}{3}] \tan \alpha + B' [(\ell^4 + h^4) x_m$$

$$(\frac{4\ell^5}{5} + \frac{8h^5}{15})] \tan^3 \alpha + 16C' [(\frac{\ell^6}{6} + \frac{h^6}{3}) x_m$$

$$- (\frac{\ell^7}{7} + \frac{4h^7}{21})] \tan^5 \alpha \qquad (9A)$$

and for the ogive-cylinder

$$\int_0^{\ell} r\, C_{D_c} (x_m - x) dx = A' [\frac{\ell^2 x_m}{2} - \frac{\ell^3}{3}] \tan \alpha + B' [(\ell^4 + \frac{3h^4}{4} + \log 2) x_m$$

$$- (\frac{4\ell^5}{5} + \frac{36h^5}{5} + 16h \log h)] \tan^3 \alpha + 16C' [(\frac{\ell^6}{6} + \frac{h^4}{24}) x_m$$

$$- (\frac{\ell^7}{7} - \frac{h^7}{42})] \tan^5 \alpha \qquad (10A)$$

These expressions simplify for the case $x_m = \ell$, for the moment coefficient C_{M_B}, to

$$\int_0^{\ell} r\, C_{D_c}(\ell - x)dx = A'\frac{\ell^3}{6}\tan\alpha + B'\left[\frac{\ell^5}{5} + \ell h^4 - \frac{8h^5}{15}\right]\tan^3\alpha$$

$$+ 16C'\left[\frac{\ell^7}{42} + \frac{\ell h^6}{3} - \frac{4h^7}{21}\right]\tan^5\alpha \qquad (11A)$$

for the cone, and

$$\int_0^{\ell} r\, C_{D_c}(\ell - x)dx = A'\frac{\ell^3}{6}\tan\alpha + B'\left[\frac{\ell^5}{5} + \frac{3\ell h^4}{4} + \ell \log 2\right.$$

$$\left. - \frac{36h^5}{5} - 16h \log h\right]\tan^5\alpha + 16C'\left[\frac{\ell^7}{42} + \frac{\ell h^4}{24} + \frac{h^7}{42}\right]\tan^5\alpha \qquad (12A)$$

for the ogive.

The powers of $\tan\alpha$ will combine with $\sin^2\alpha$ to give, to seventh degree terms:

$$\sin^2\alpha \tan\alpha = \alpha^3 + \frac{\alpha^7}{15} + - - - \qquad (13A)$$

$$\sin^2\alpha \tan^3\alpha = \alpha^5 + \frac{2\alpha^7}{3} + - - - \qquad (14A)$$

$$\sin^2\alpha \tan^5\alpha = \alpha^7 + - - - \qquad (15A)$$

These may be substituted in Eq. 3A, 4A, 7A, and 11A to give, for cone-cylinders,

$$\Delta C_N = \frac{2C_{D_c}}{A}\left[\frac{A'\ell^2}{2}\alpha^3 + B'(\ell^4 + h^4)\alpha^5 + \left(16C'\left\{\frac{\ell^6}{6} + \frac{h^6}{3}\right\} + \frac{2B'}{3}\left\{\ell^4 + h^4\right\} + \frac{A'}{30}\ell^2\right)\alpha^7\right] \qquad (16A)$$

$$\Delta C_{M_B} = \frac{2C_{D_c}}{A}\left[\frac{A'\ell^3}{6}\alpha^3 + B'\left(\frac{\ell^5}{5} + \ell h^4 - \frac{8h^5}{15}\right)\alpha^5 + \left(16C'\left\{\frac{\ell^7}{42} + \frac{\ell h^6}{3} \quad \frac{4h^7}{21}\right\} + \frac{2B'}{3}\left\{\ell^5 + \ell h^4 - \frac{8h^5}{15}\right\} + \frac{A'}{90}\ell^3\right)\alpha^7\right] \qquad (17A)$$

where C_{D_c} is now the steady-state value of the cylinder cross flow drag coefficient.

A similar substitution for ogive-cylinders yields from Eq. 3A, 4A, 8A, and 12A

$$\Delta C_N = \frac{2C_{D_c}}{A}\left[\frac{A'\ell^2}{2}\alpha^3 + B'\left(\ell^4 + \frac{3h^4}{4} + \log 2\right)\alpha^5 + \left(16C'\left\{\frac{\ell^6}{6} + \frac{h^4}{24}\right\} + \frac{2B'}{3}\left\{\ell^4 + \frac{3h^4}{4} + \log 2\right\} + \frac{A'\ell^2}{30}\right)\alpha^7\right] \quad (18A)$$

$$\Delta C_{M_B} = -\frac{2C_{D_c}}{A}\left[\frac{A'\ell^3}{6}\alpha^3 + B'\left(\frac{\ell^5}{5} + \frac{3\ell h^4}{4} + \ell \log 2 - \frac{36h^5}{5} - 16h \log h\right)\alpha^5 + \left(16C'\left\{\frac{\ell^7}{42} + \frac{\ell h^4}{24} + \frac{h^7}{42}\right\} + \frac{2B'}{3}\left\{\frac{\ell^5}{5} + \frac{3\ell h^4}{4} + \ell \log 2 - \frac{36h^5}{5} - 16h \log h\right\} + \frac{A'\ell^3}{90}\right)\alpha^7\right] \quad (19A)$$

Many of the terms in 16A through 19A may be neglected, especially for $h << \ell$.

As an example of the use of the above equations, the viscous increments for a 7 caliber cone-cylinder, $\ell = 7$ and $h = 2$, become, with $C_{D_c} = 0.35$

$$\Delta C_N = \frac{2.8}{\pi}\left[12\alpha^3 - 13.5\alpha^5 + 1.22\alpha^7\right] \quad (20A)$$

$$\Delta C_{M_B} = \frac{2.8}{\pi}[28\alpha^3 - 19.35\alpha^5 - 1.55\alpha^7] \qquad (21A)$$

The ogive-cylinder with $\ell = 14$, $h = 3.5$, gives

$$\Delta C_N = \frac{2.8}{\pi}[48\alpha^3 - 216\alpha^5 + 460\alpha^7] \qquad (22A)$$

$$\Delta C_{M_B} = \frac{2.8}{\pi}[224\alpha^3 - 591\alpha^5 + 824\alpha^7] \qquad (23A)$$

The front multiplying factor must be changed to $\frac{9.6}{\pi}$ for a laminar boundary layer.

Appendix B

COMPARISON OF THEORIES WITH EXPERIMENTAL DATA

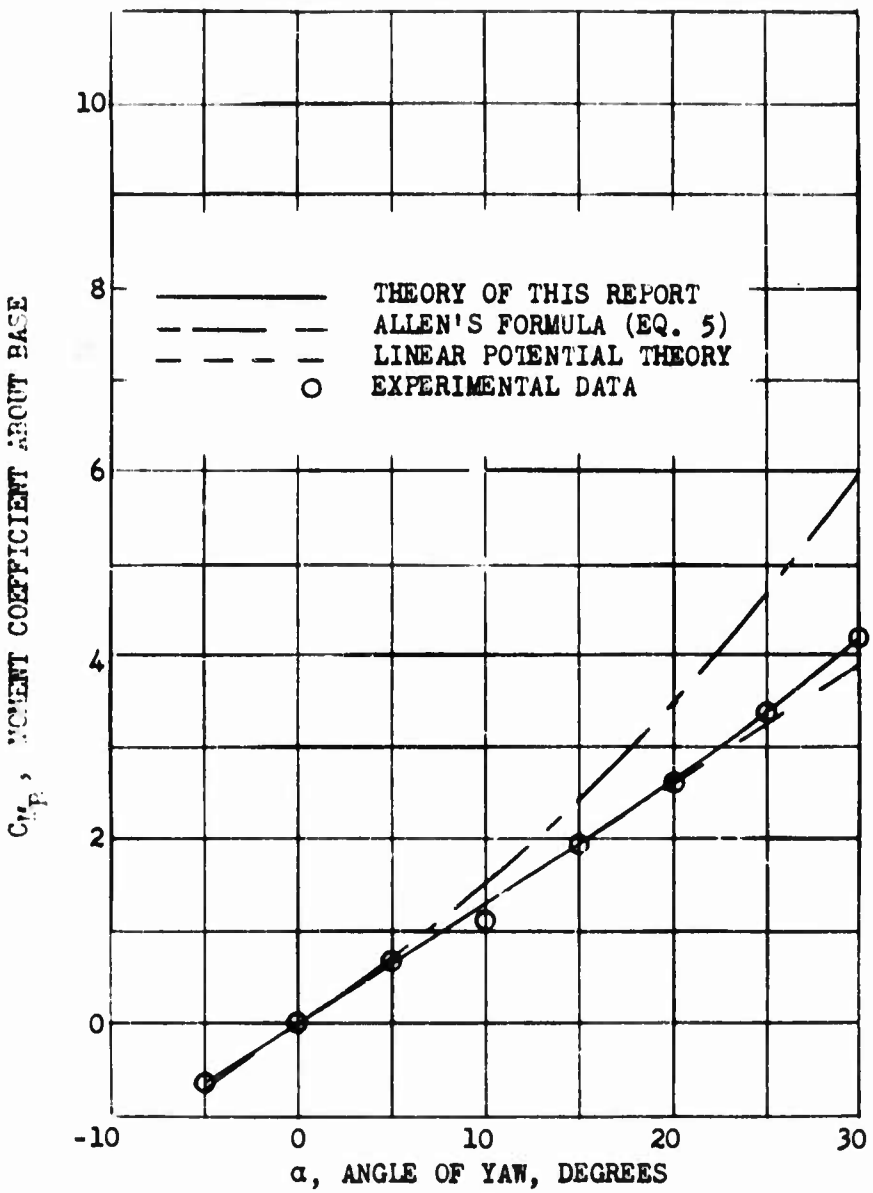

FIG. 6. PITCHING MOMENT COEFFICIENT FOR A SECANT-OGIVE-CYLINDER AT M = 0.26.

5 CALIBER LENGTH
2 CALIBER HEAD LENGTH
Re = 4.2×10^6

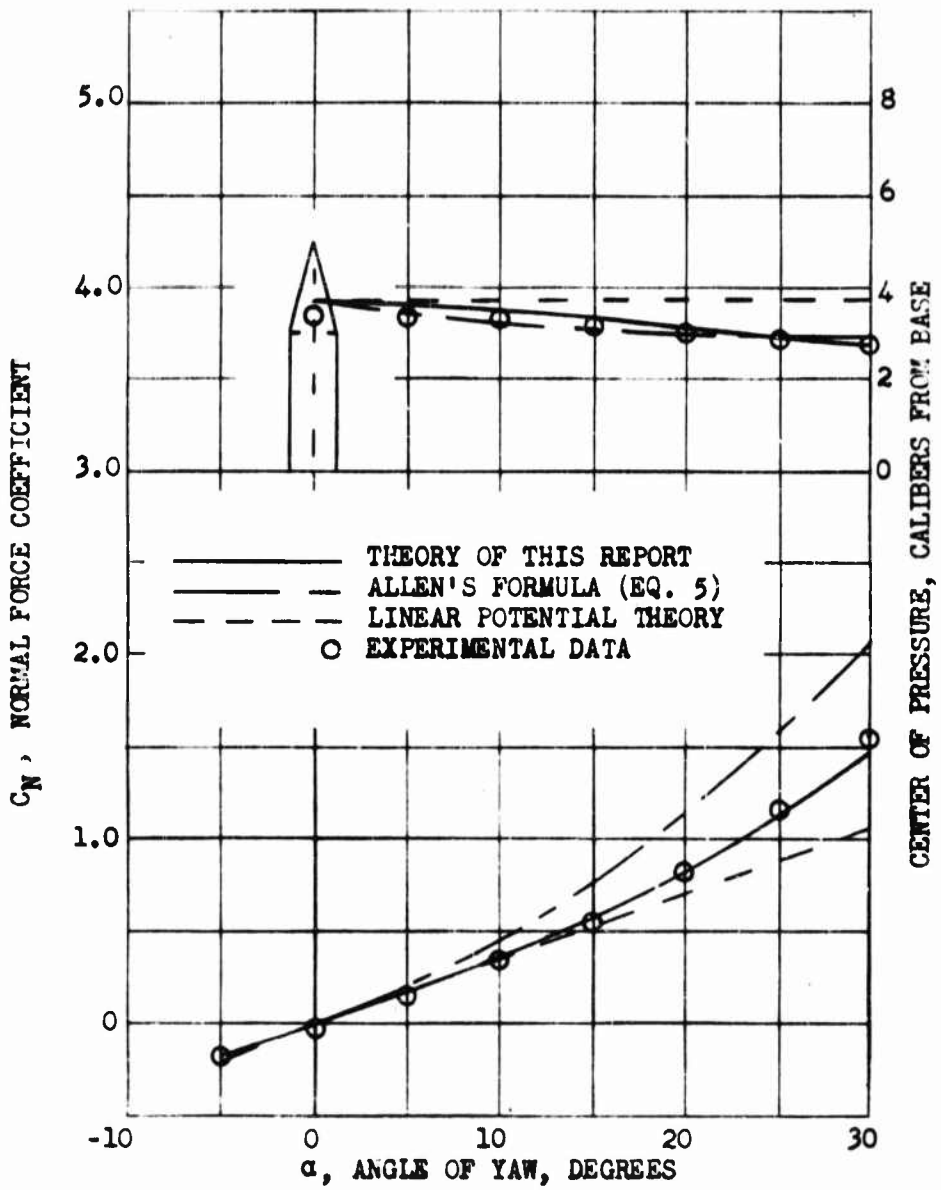

FIG. 7. NORMAL FORCE COEFFICIENT AND CENTER OF PRESSURE FOR A SECANT-OGIVE-CYLINDER AT M = 0.26.

5 CALIBER LENGTH
2 CALIBER HEAD LENGTH
Re = 4.2×10^6

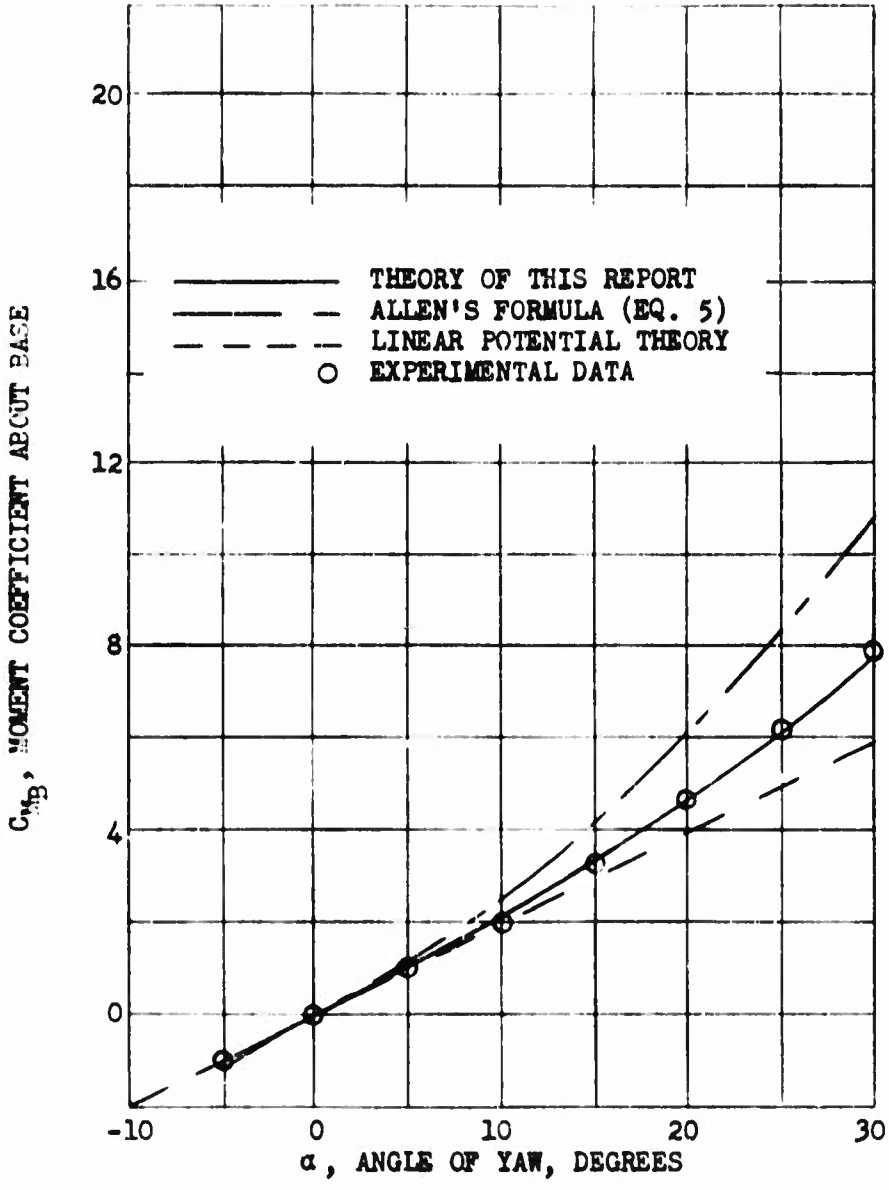

FIG. 8. PITCHING MOMENT COEFFICIENT FOR A SECANT-OGIVE-CYLINDER AT M = 0.26.

7 CALIBER LENGTH
2 CALIBER HEAD LENGTH
$Re = 5.9 \times 10^6$

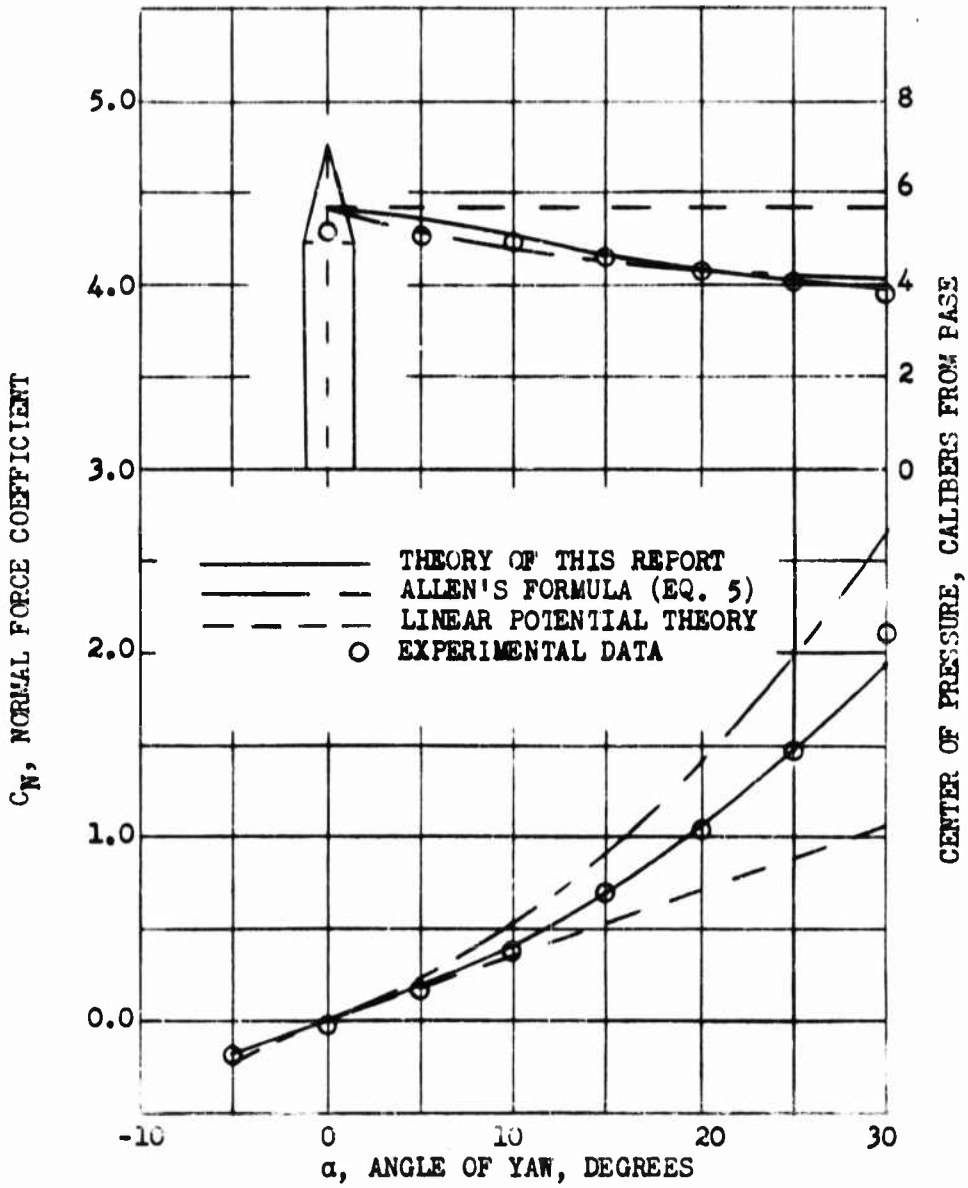

FIG. 9. NORMAL FORCE COEFFICIENT AND CENTER OF PRESSURE FOR A SECANT-OGIVE-CYLINDER AT M = 0.26

7 CALIBER LENGTH
2 CALIBER HEAD LENGTH
Re = 5.9×10^6

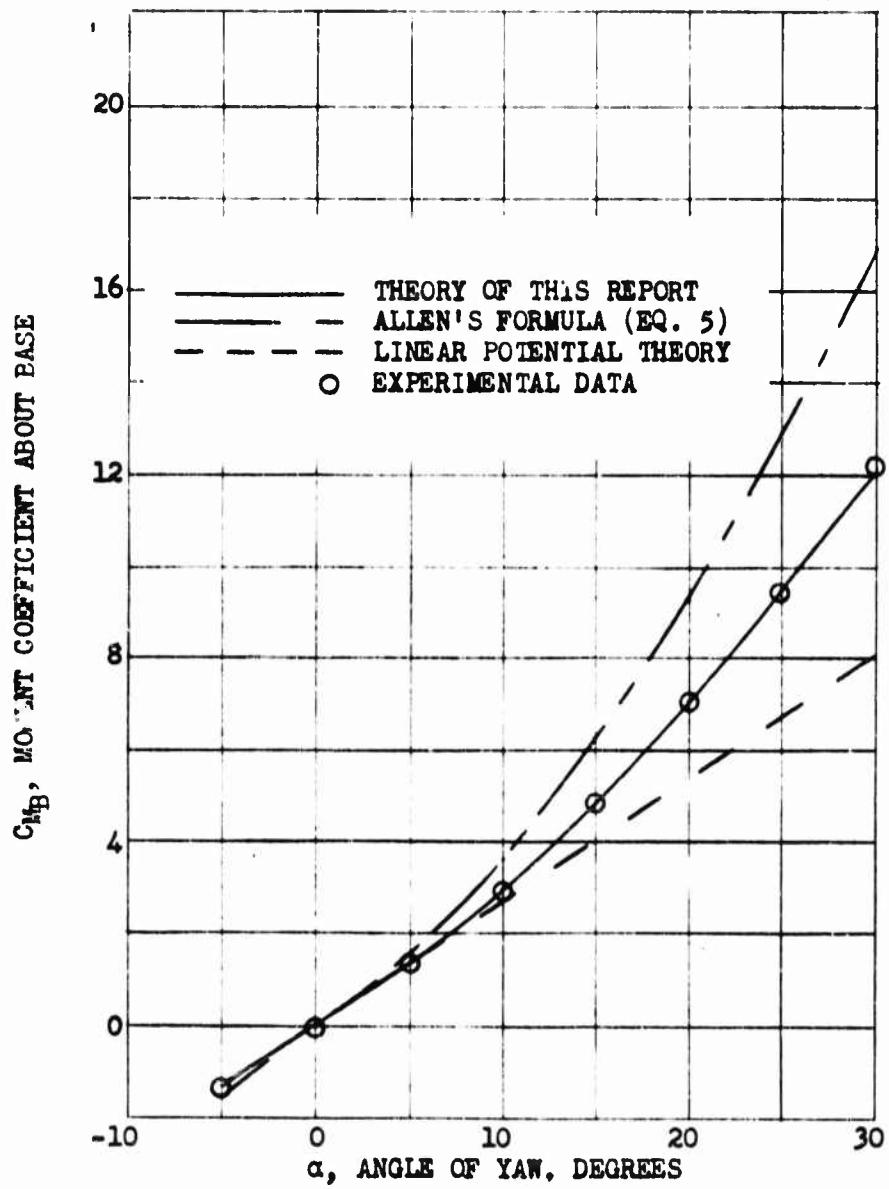

FIG. 10. PITCHING MOMENT COEFFICIENT FOR A SECANT-OGIVE-CYLINDER AT M = 0.26.

9 CALIBER LENGTH
2 CALIBER HEAD LENGTH
Re = 7.6×10^6

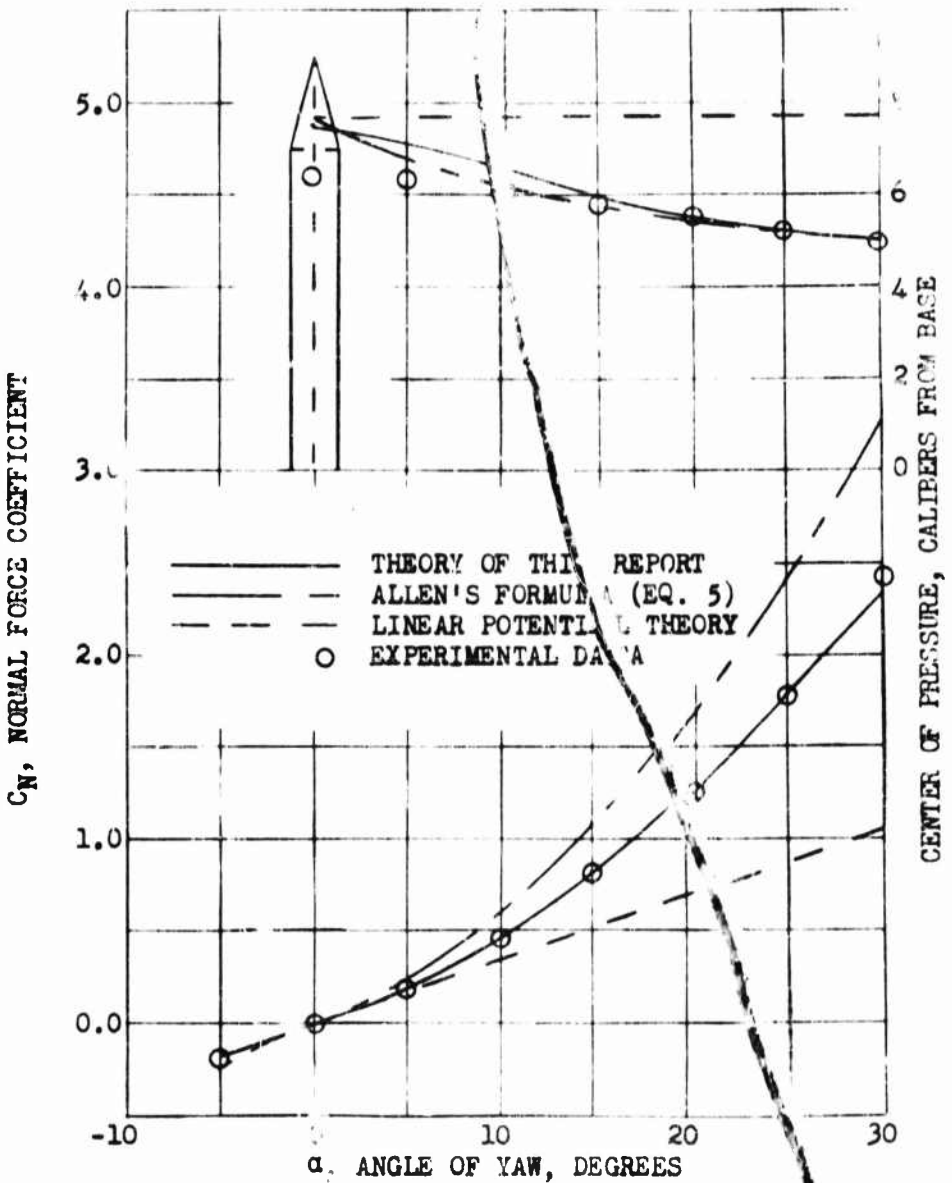

FIG. 11. NORMAL FORCE COEFFICIENT AND CENTER OF PRESSURE FOR A SECANT-OGIVE-CYLINDER AT M = 0.26.

9 CALIBER LENGTH
2 CALIBER HEAD LENGTH
Re = 7.6 x 10^6

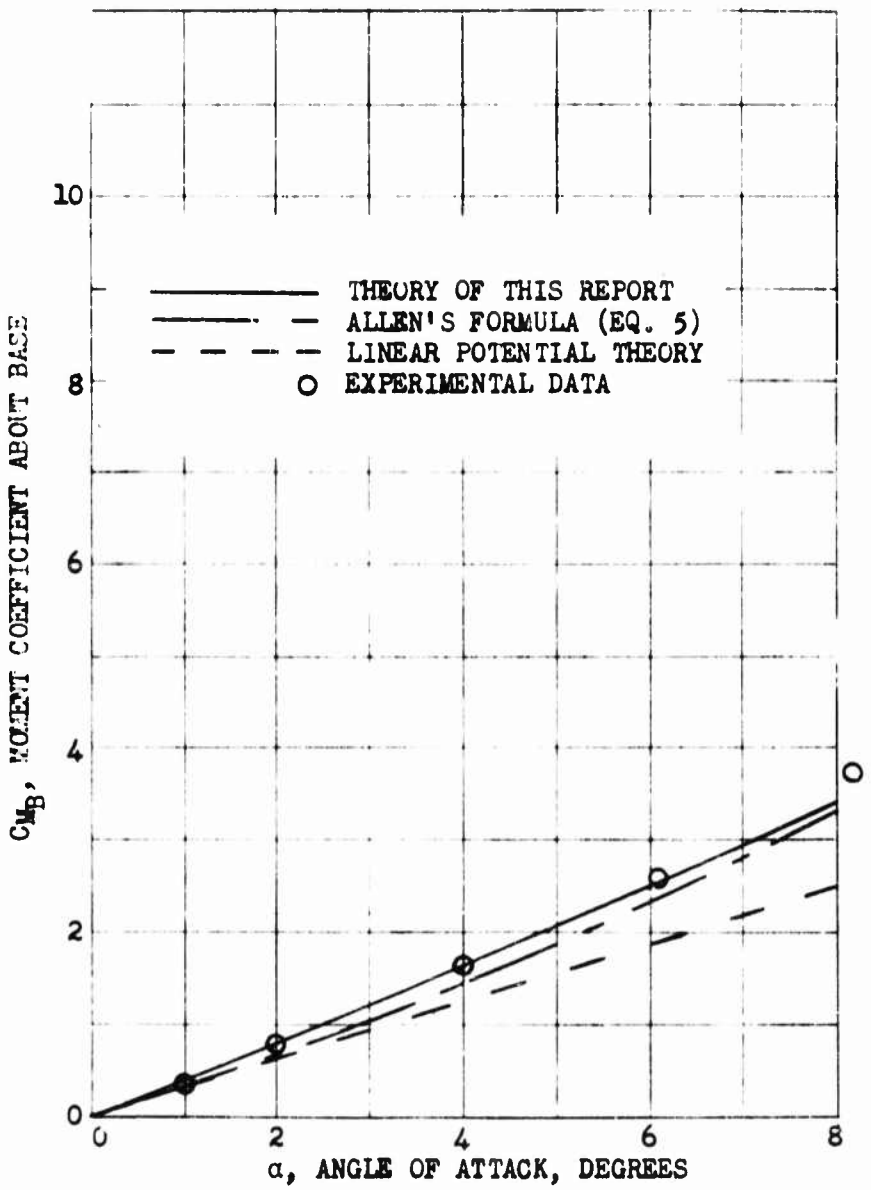

FIG. 12. PITCHING MOMENT COEFFICIENT FOR A TANGENT-OGIVE-CYLINDER AT M = 1.56.

10 CALIBER LENGTH
2.5 CALIBER HEAD LENGTH
Re = 4×10^6

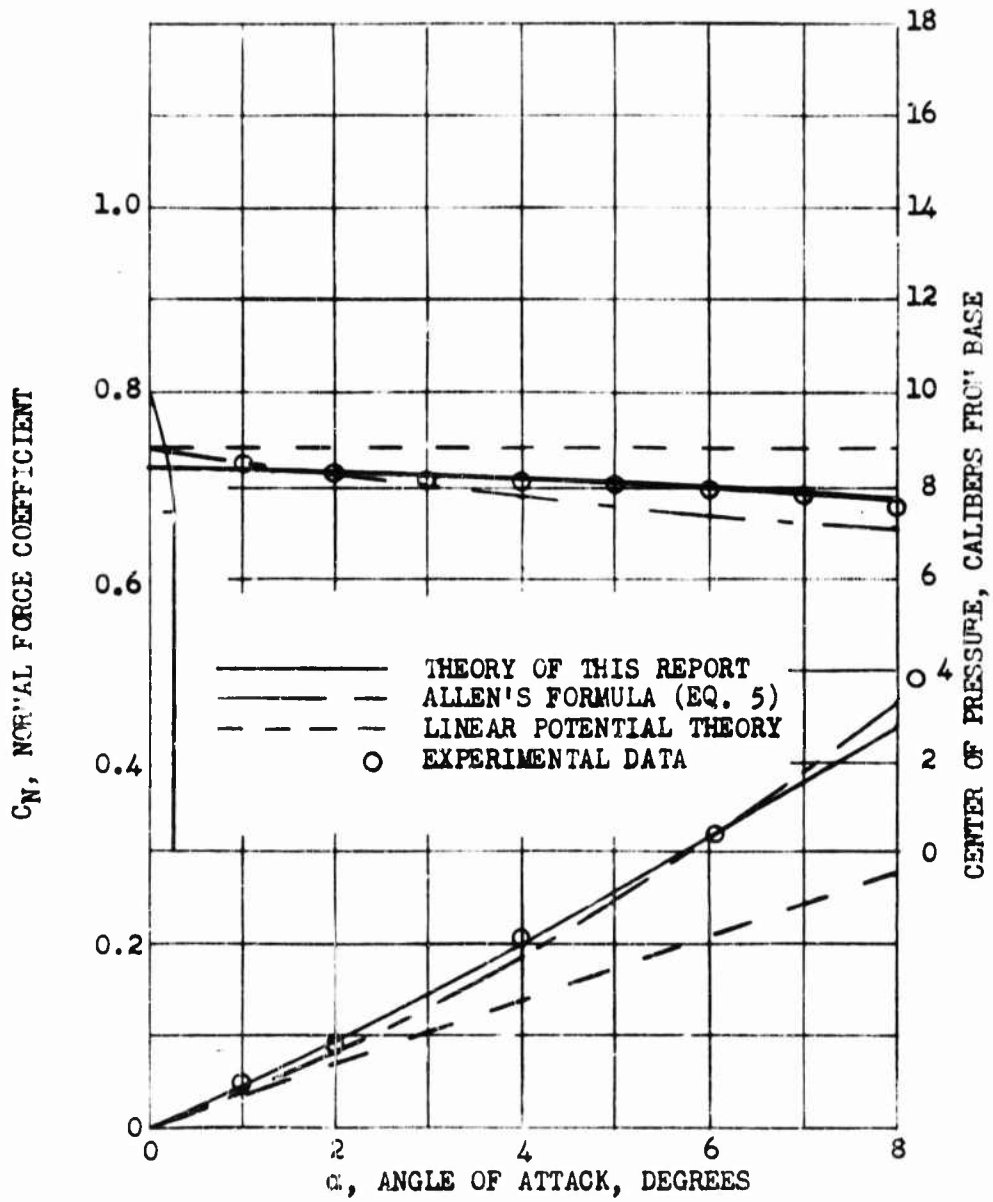

FIG. 13. NORMAL FORCE COEFFICIENT AND CENTER OF PRESSURE FOR A TANGENT-OGIVE-CYLINDER AT M = 1.56.

10 CALIBER LENGTH
2.5 CALIBER HEAD LENGTH
Re = 4 x 10^6

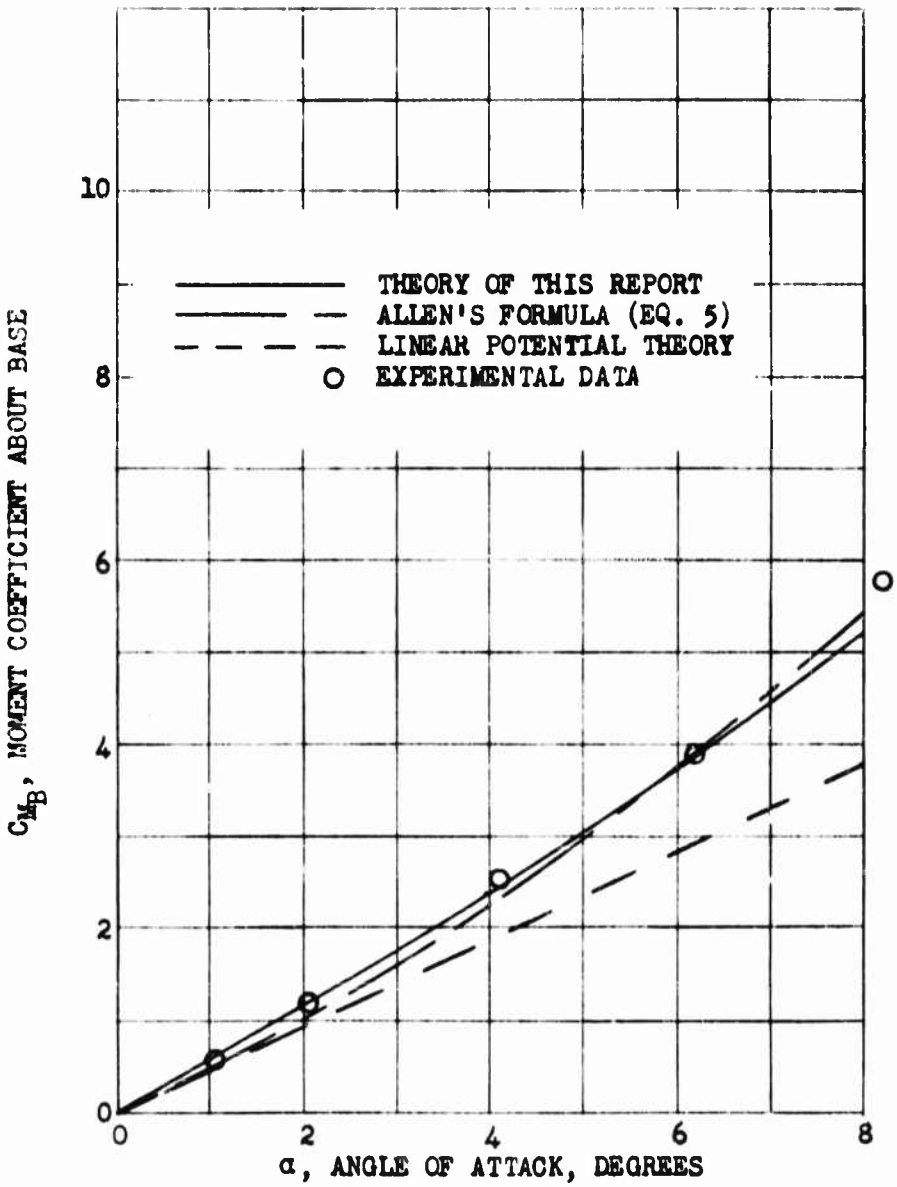

FIG. 14. PITCHING MOMENT COEFFICIENT FOR A TANGENT-OGIVE-CYLINDER AT M = 1.56.

14 CALIBER LENGTH
2.5 CALIBER HEAD LENGTH
Re = 5.6×10^6

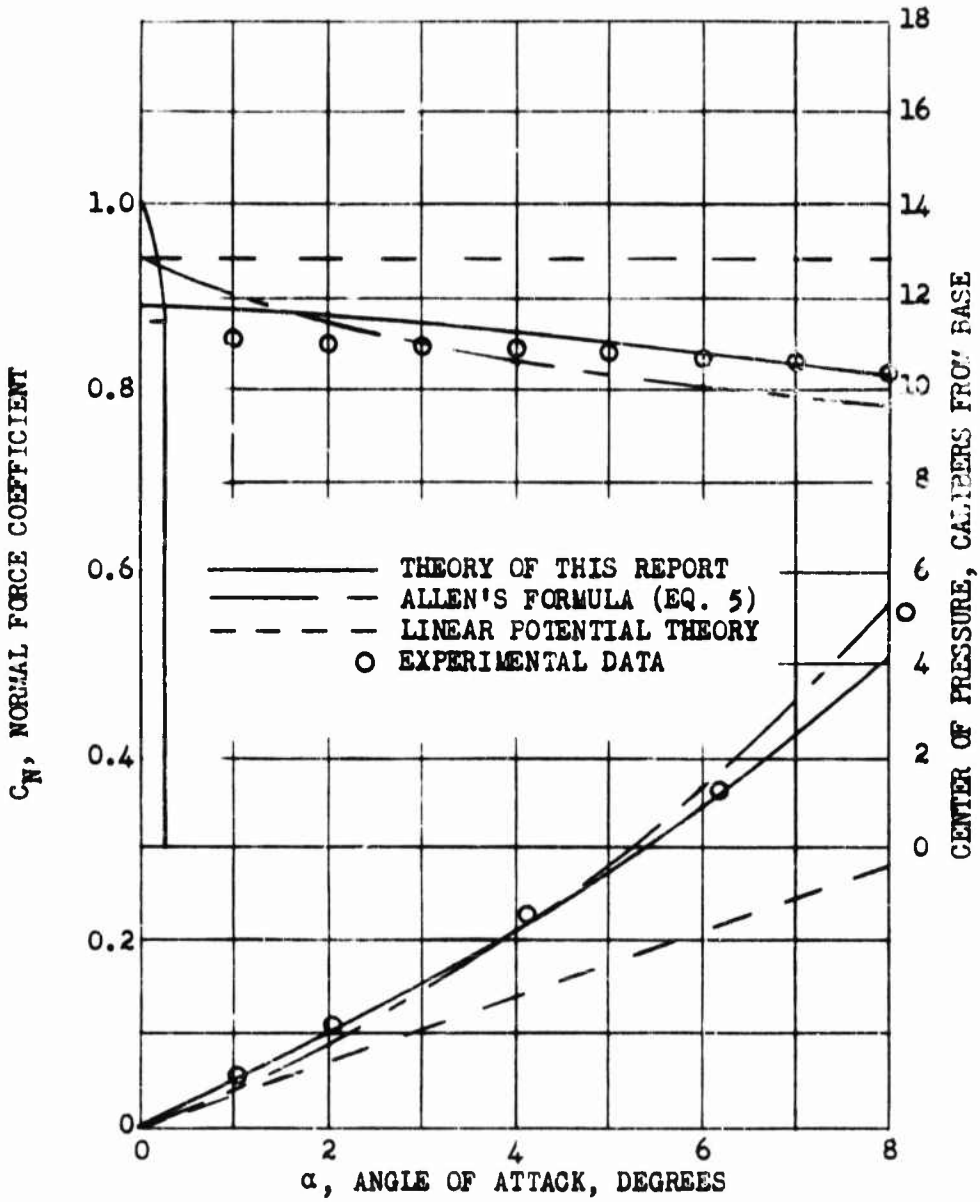

FIG. 15. NORMAL FORCE COEFFICIENT AND CENTER OF PRESSURE FOR A TANGENT-OGIVE-CYLINDER AT M = 1.56.

14 CALIBER LENGTH
2.5 CALIBER HEAD LENGTH
Re = 5.6×10^6

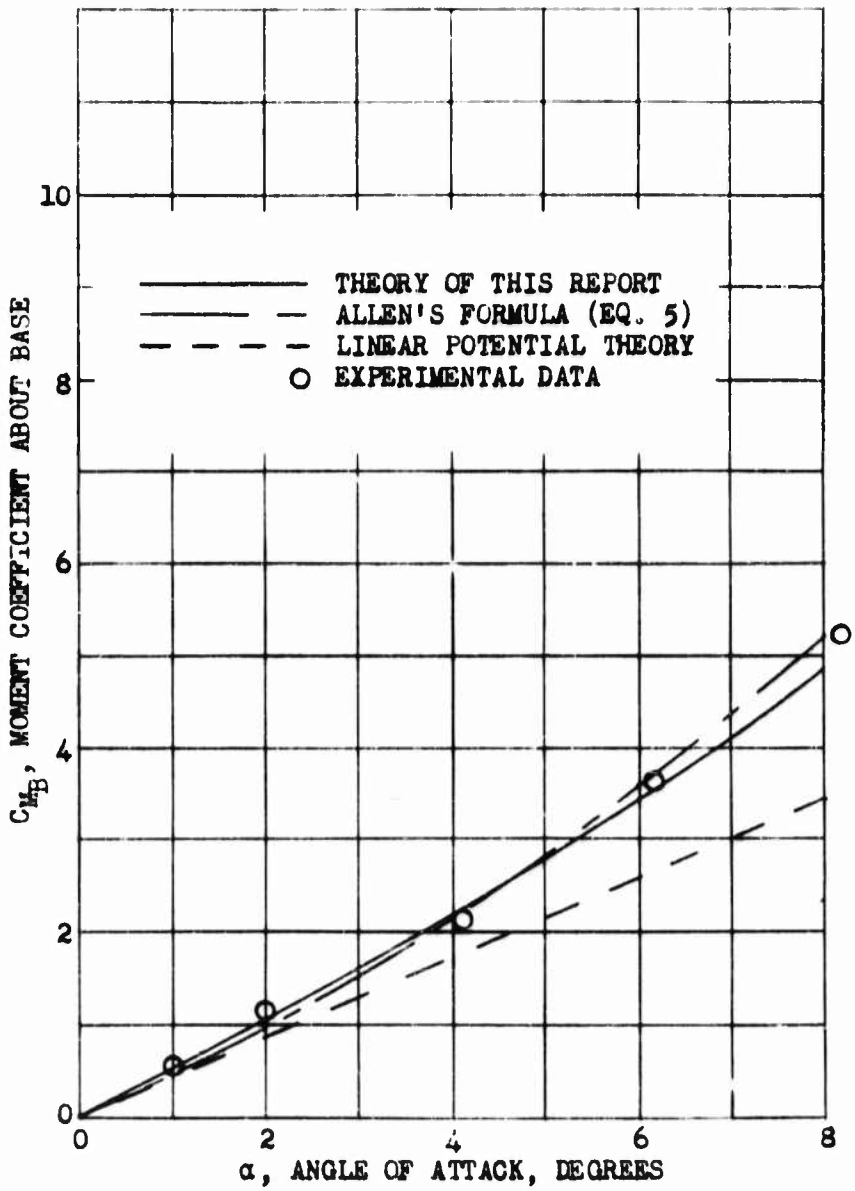

FIG. 16. PITCHING MOMENT COEFFICIENT FOR A TANGENT-OGIVE-CYLINDER AT M = 1.56.

14 CALIBER LENGTH
3.5 CALIBER HEAD LENGTH
Re = 5.6×10^6

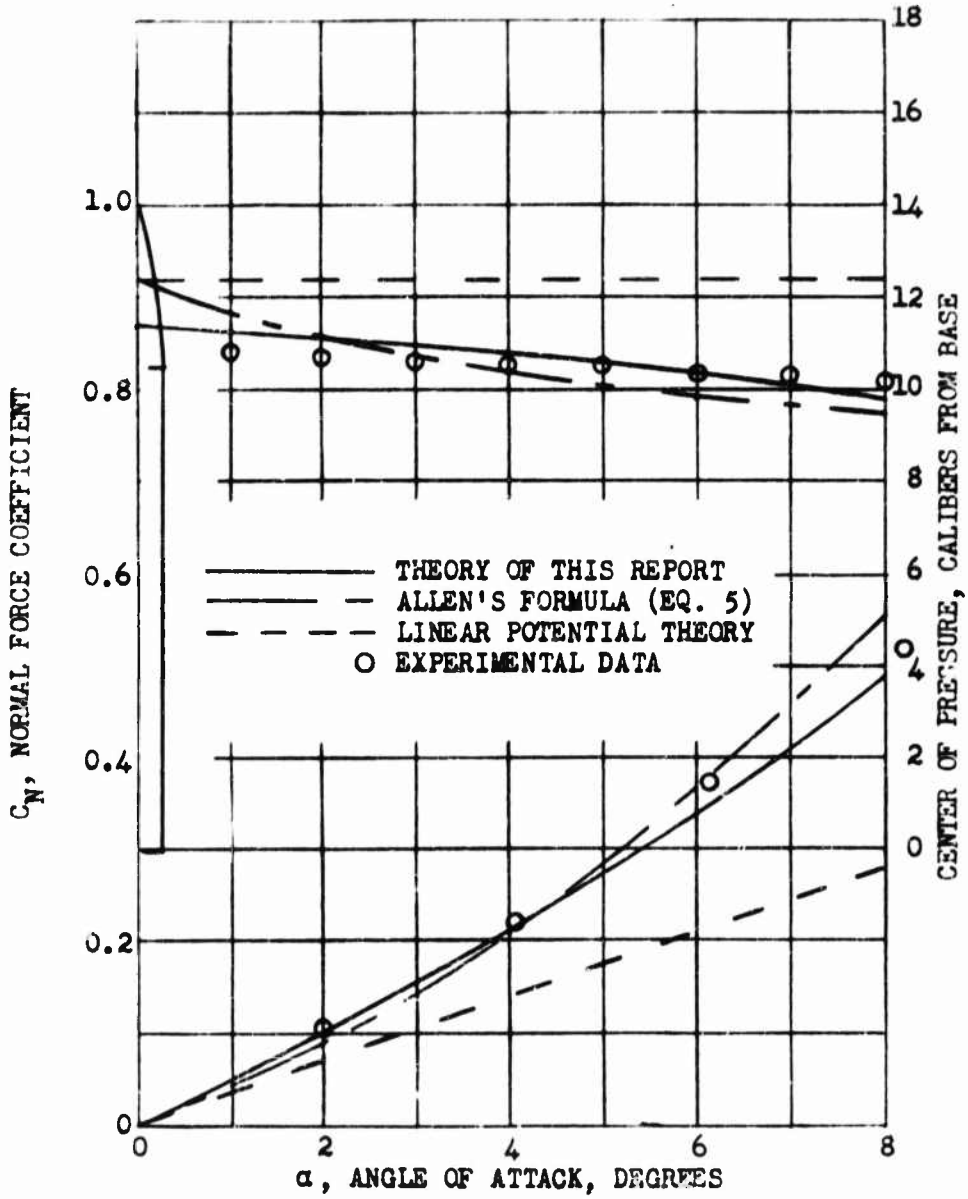

FIG. 17. NORMAL FORCE COEFFICIENT AND CENTER OF PRESSURE FOR A TANGENT-OGIVE-CYLINDER AT M = 1.56.

14 CALIBERS LENGTH
3.5 CALIBERS HEAD LENGTH
Re = 5.6×10^6

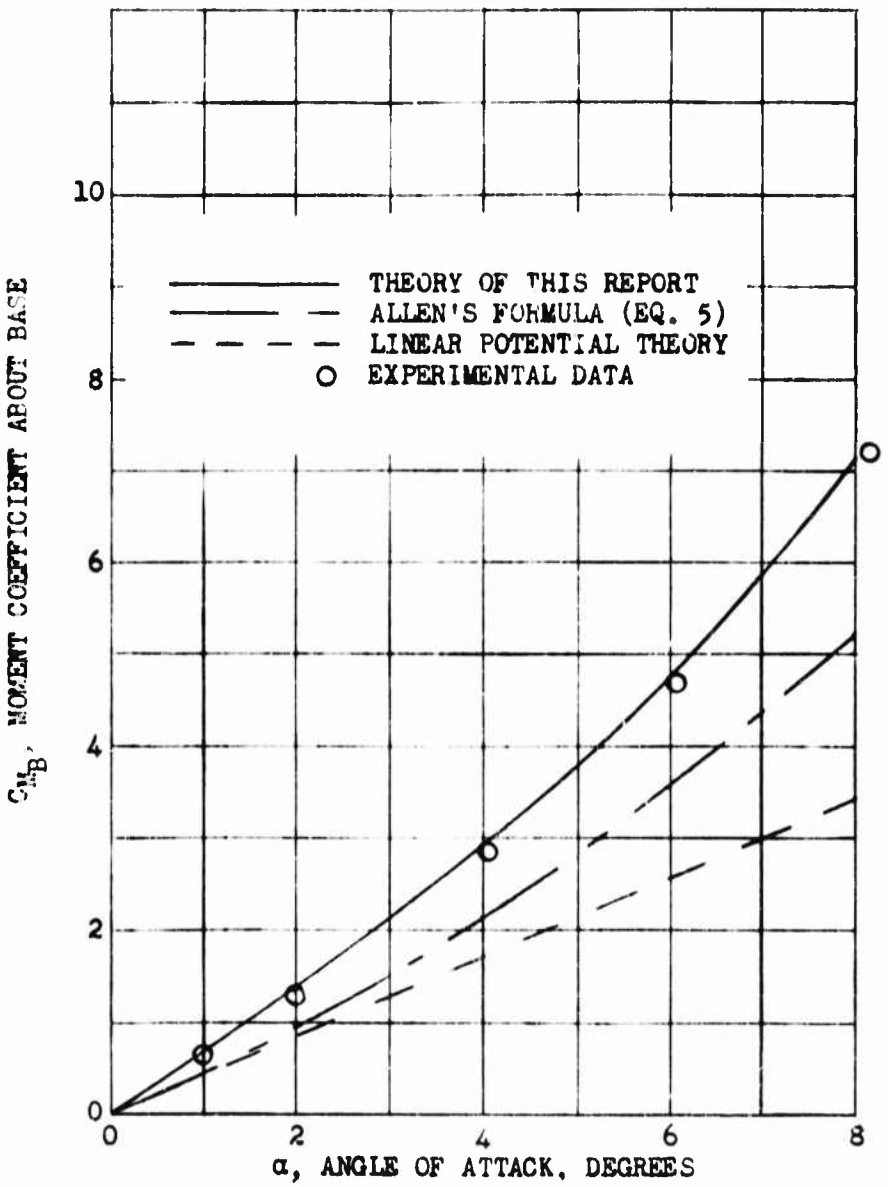

FIG. 18. PITCHING MOMENT COEFFICIENT FOR A TANGENT-OGIVE-CYLINDER AT M = 2.87.

14 CALIBER LENGTH
3.5 CALIBER HEAD LENGTH
Re = 3.7×10^6

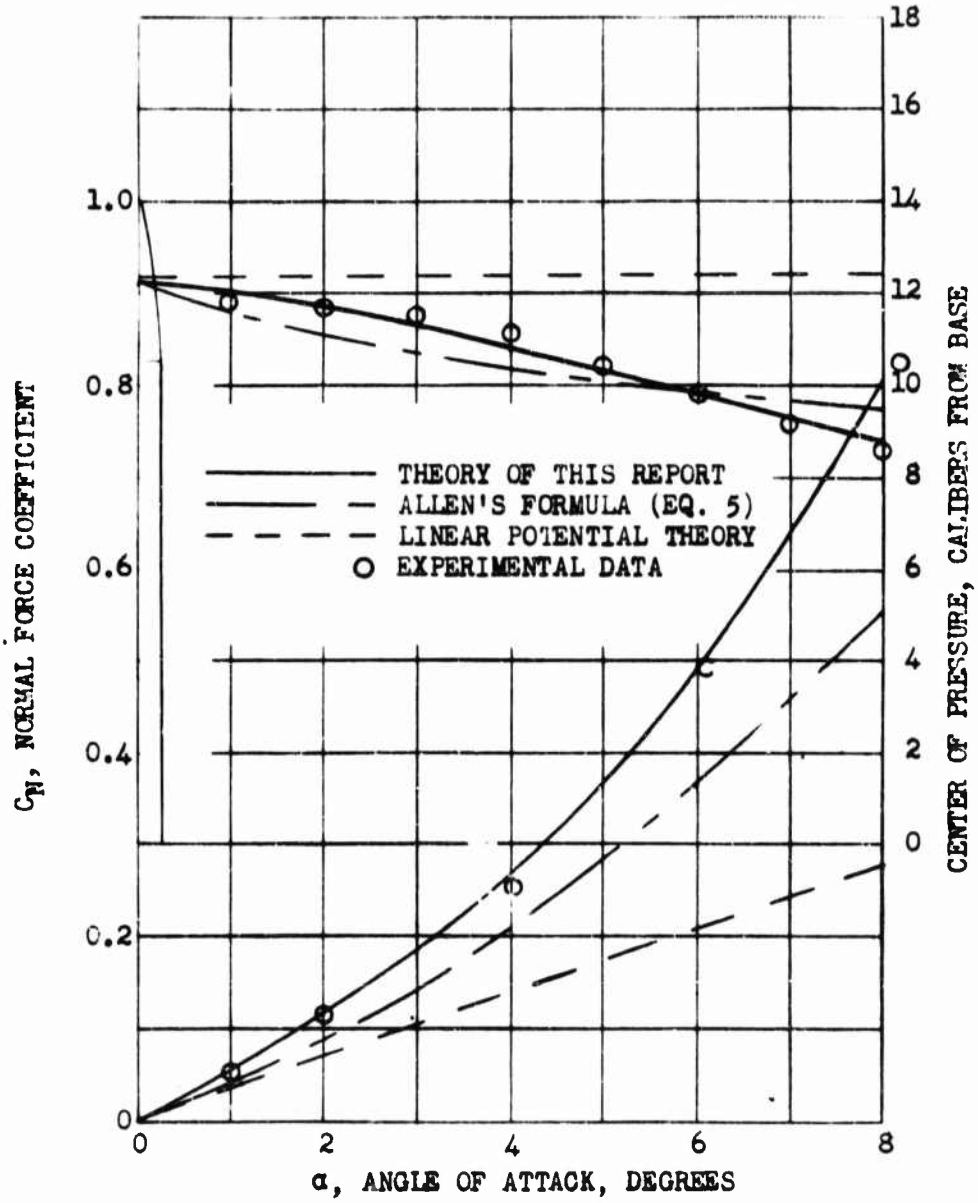

FIG. 19. NORMAL FORCE COEFFICIENT AND CENTER OF PRESSURE FOR A TANGENT-OGIVE-CYLINDER AT M = 2.37.

14 CALIBER LENGTH
3.5 CALIBER HEAD LENGTH
Re = 3.7×10^6

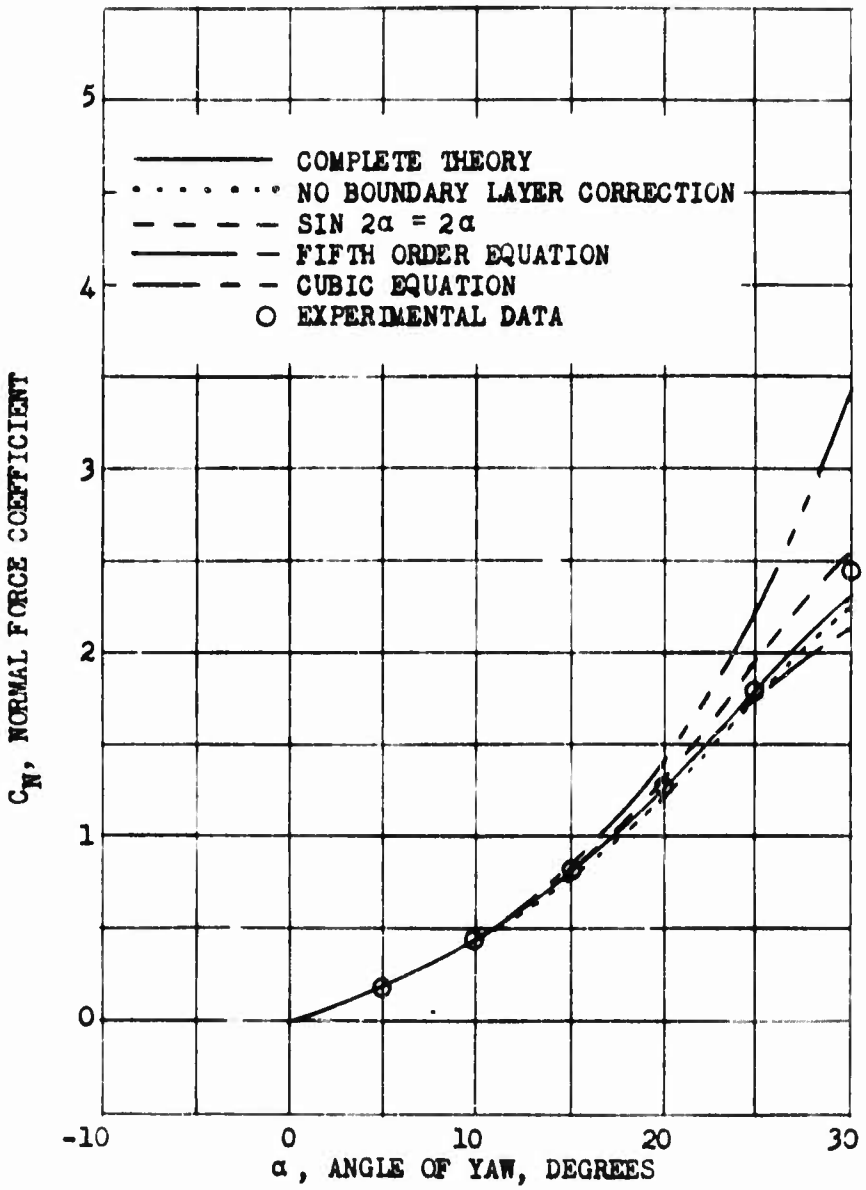

FIG. 20. NORMAL FORCE COEFFICIENT FOR A NINE CALIBER BODY, USING DIFFERENT APPROXIMATIONS.

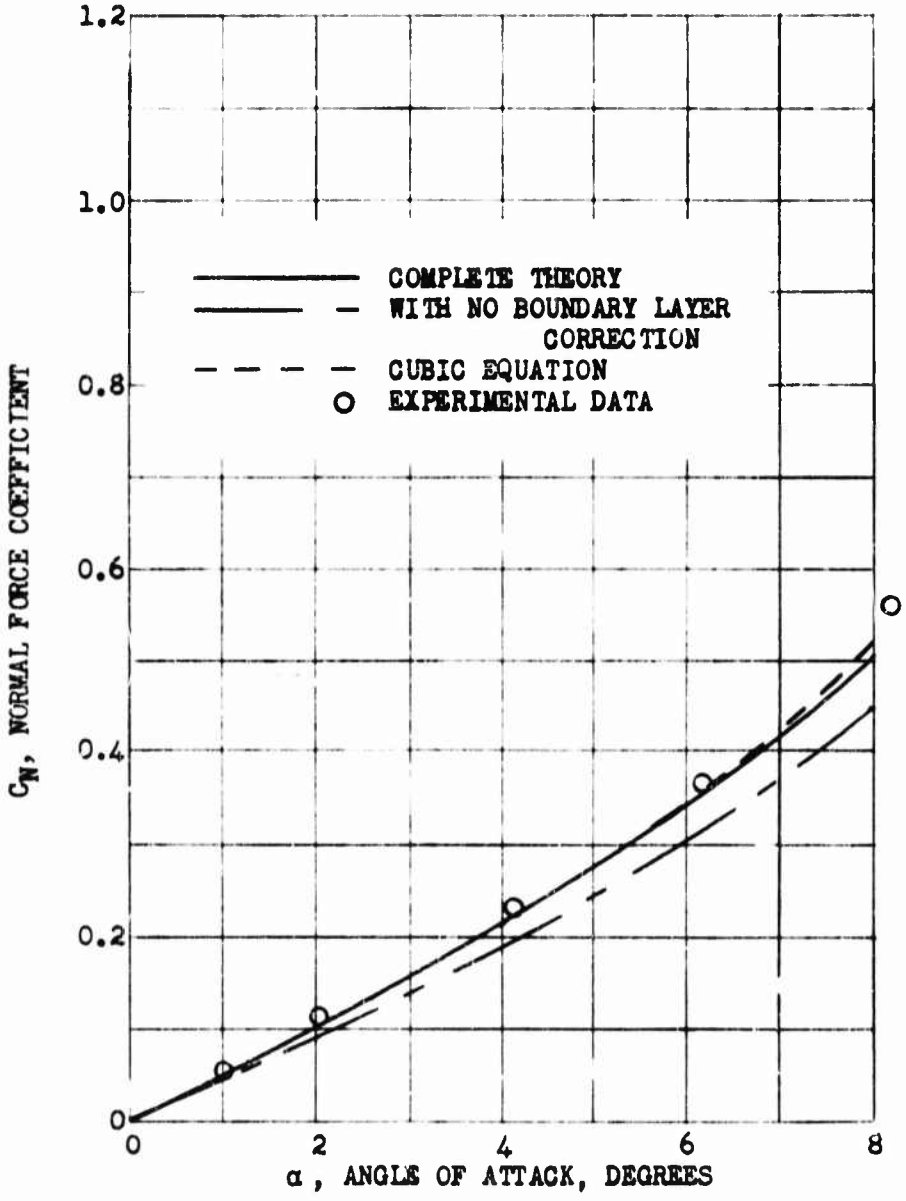

FIG. 21. NORMAL FORCE COEFFICIENT FOR A FOURTEEN CALIBER BODY WITH TURBULENT BOUNDARY LAYER, USING DIFFERENT APPROXIMATIONS.

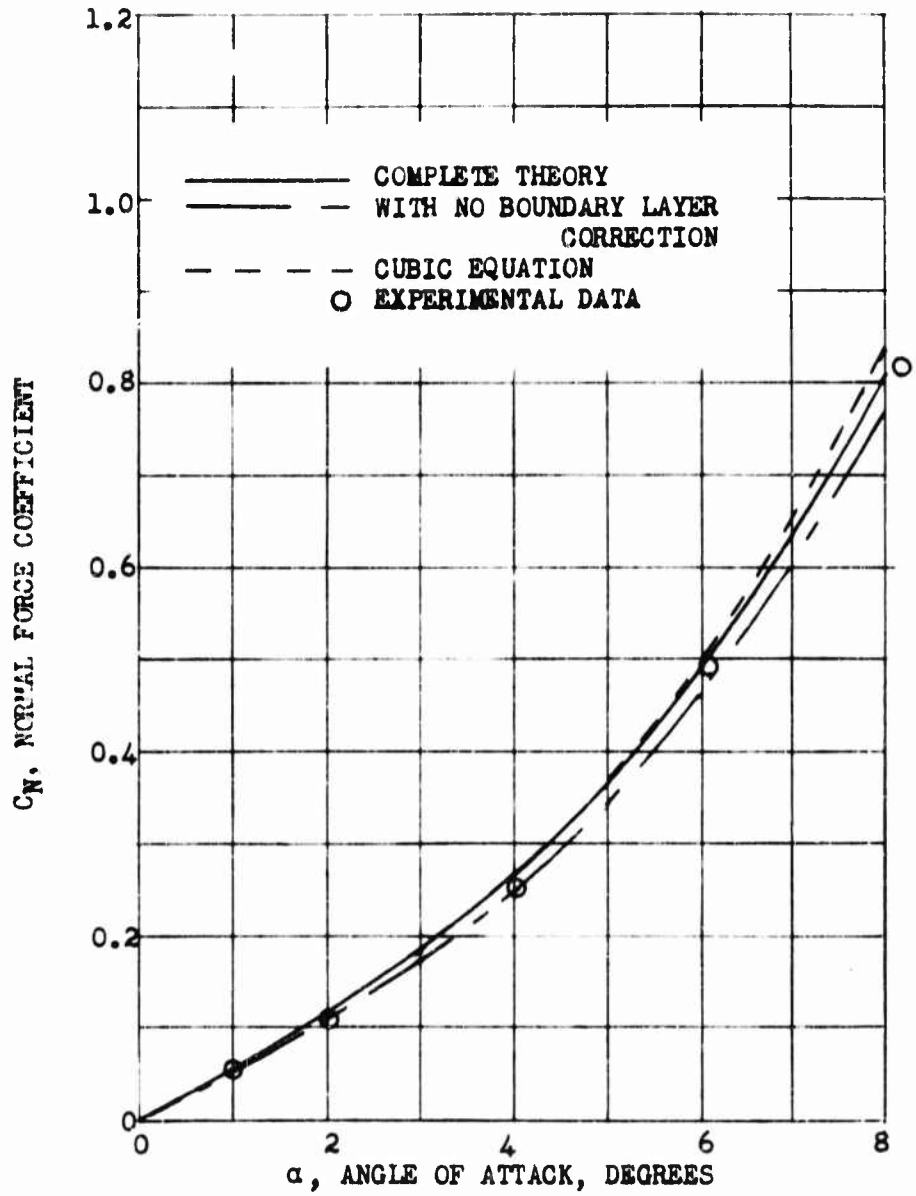

FIG. 22. NORMAL FORCE COEFFICIENT FOR A FOURTEEN CALIBER BODY WITH LAMINAR BOUNDARY LAYER, USING DIFFERENT APPROXIMATIONS.

NOMENCLATURE

A	Reference area for defining coefficients
A_p	Planform area of body
A', B', C'	Polynomial coefficients (Eq. 13)
C_{D_c}	Drag coefficient of cylinder in a crossflow $\frac{D_c}{\frac{\rho V_c^2}{2} A_p}$
C_L	Lift coefficient $\frac{L}{qA}$
C_M	Pitching moment coefficient $\frac{M_P}{qAd}$
C_{M_B}	Pitching moment coefficient about base
C_N	Normal force coefficient $\frac{N}{qA}$
D, E, F	Polynomial coefficients (Eq. 15)
D_c	Crossflow drag on a cylinder
K	Parameter for turbulent boundary layer (Eq. 20)
L	Lift force
M	Mach number
M_c	Mach number of crossflow
M_P	Pitching moment
N	Normal force
Re	Reynolds number

Re_c	Reynolds number of crossflow
S	Cross-sectional area of body at station x
S_B	Cross-sectional area at base
S_B'	Base area, corrected for boundary layer
U	Free stream velocity
V	Volume of body
V'	Volume, corrected for boundary layer
V_c	Velocity of crossflow
a	Speed of sound
d	Diameter of body (= 1 caliber)
h	Head length in calibers
$k_2 - k_1$	Apparent mass correction from Munk's theory
ℓ	Fineness ratio (body length in calibers)
q	Dynamic pressure $\rho \frac{U^2}{2}$
r	Body radius at station x
t	Time in seconds
u	Local axial velocity in boundary layer
x	Axial coordinate in calibers
x_c	Axial position of body centroid

x_m	Center of moments
α	Angle of attack
β	$\sqrt{M^2 - 1}$
δ	Boundary layer thickness
δ^*	Boundary layer displacement thickness
Δ	Parameter for laminar boundary layer (Eq. 17, 18)
η	Drag correction factor for finite length cylinder
ν	Kinematic viscosity of air
ρ	Air density

REFERENCES

1. National Advisory Committee for Aeronautics. The Aerodynamic Forces on Airship Hulls, by Max M. Munk. NACA, 1924 (NACA Report 184).

2. ------. Estimation of the Forces and Moments on Inclined Bodies of Revolution of High Fineness Ratio, by H. Julian Allen. Washington, November 14, 1949 (NACA RM A9I26) CONFIDENTIAL.

3. ------. Characteristics of Flow Over Inclined Bodies of Revolution, by H. Julian Allen and Edward W. Perkins. Washington, March 5, 1951 (NACA RM A50L07) CONFIDENTIAL.

4. ------. A Study of Effects of Viscosity on Flow Over Slender Inclined Bodies of Revolution, by H. Julian Allen and Edward W. Perkins. Moffett Field, Calif., 1951 (NACA Report 1048).

5. Ward, G. N. Supersonic Flow Past Slender Pointed Bodies. QUART J MECH APPL MATH, Vol 2, Part I, March 1949, pp. 75-97.

6. Goldstein, S. Modern Developments in Fluid Dynamics, Oxford, 1938.

7. Massachusetts Institute of Technology. Forces on Slender Bodies at Angle of Attack, by J. A. F. Hill. Naval Supersonic Laboratory, M. I. T., May 9, 1950 (MIT NSL R-a 100-59) CONFIDENTIAL.

8. National Advisory Committee for Aeronautics. Pressure Distribution in Nonuniform Two-Dimensional Flow, by M. Schwabe. Washington, January 1943 (NACA TM 1039).

9. Lamb, Horace. Hydrodynamics. Sixth Edition, Dover Publications, New York, 1945

10. Van Dyke, Milton D. First- and Second Order Theory of Supersonic Flow Past Bodies of Revolution. J AERONAUT SCI, Vol 18, No. 3, March 1951. pp. 161-178.

11. Naval Ordnance Test Station, Inyokern. Some Results of a Systematic Theoretical Pressure Distribution Program on Bodies of Revolution, by Eldon L. Dunn. China Lake, Calif., 8 April 1953 (NOTS TM-919).

DISTRIBUTION

Code 01
P0102
12
1425
15
P16
17
1702
174
30
35
3527
40
401
403
50
501
503
5036 (3)
507
5507 (3)
P80
P9509 (22)
NACA Langley Field, Technical Library
Ames Aeronautical Laboratory
H. Julian Allen (1)
Edward W. Perkins (1)
Technical Library (1)
Massachusetts Institute of Technology
Mr. J. A. F. Hill, Naval Supersonic Laboratory (1)
Technical Library (1)
Aberdeen Proving Ground, Ballistics Research Laboratory
Mr. C. L. Poor (1)
Mr. John Nicolaides (1)

Mr. Marvin L. Luther
Dr. Ralph H. Upson
Aercon, Inc.
5032 Files

In addition, distribution in accordance with:

a. BuOrd restr ltr Re3e-JAR:mv S78(119) of 12 Dec 50 to NOTS, NOL, and NOP

b. Buord conf ltr S78-1(119) Re3-HG:jk Ser 13774 of 8 Nov 50 to NOTS, NOL, and NOP